MSc thesis SUSD-ECE

Ecological stability in the face of climatic disturbances

a case study of a dryland ecosystem in the Moroccan High Atlas Mountains

Keywords: Moroccan Atlas Mountains, ecological stability, drought, NDVI, Landsat, time-series, change detection

Student: Angelique Vermeer (4066804), a.l.vermeer2@students.uu.nl

Supervisors: Ángeles Garcia Mayor (Utrecht University), Saskia Förster (German Research Centre for Geosciences)

Summary

Drylands suffer from land degradation due to increasing anthropogenic pressure and climate change. This threatens the existence of these valuable ecosystems and the people that live in them. The ecological stability of an ecosystem determines how it responds to disturbances. Understanding ecological stability is, therefore, crucial in preventing land degradation and designing strategies for restoration. In this study, the ecological stability of a dryland ecosystem in the Moroccan High Atlas Mountains, in the face of both a drought and a heavy flooding period, was determined. The Breaks For Additive Seasonal and Trend (BFAST) change detection methodology was used to determine breakpoints and trends in a time-series of Landsat NDVI data between 1984 and 2019. The breakpoints were classified using a newly developed typology based on the trend before and after the breakpoint. The improved typology that is introduced in this thesis, considers the statistical significance of trends and subdivides them in categories of abrupt changes that lead to an improvement of ecosystem functioning (positive breakpoints) and abrupt changes that lead to a deterioration of ecosystem functioning (negative breakpoints). Ecological stability was quantified using the resistance to abrupt changes that lead to a deterioration in ecosystem functioning and the response to climatic disturbances (i.e. the drought and the flood) as indicators. The resulting data on resistance and response to climatic disturbances were compared to data of land cover classification, overall change in vegetation cover and initial vegetation cover. The results show that ecological stability is higher in the northern part of the Ounila watershed. Ecological stability is lowest in lower-lying bare areas in the east and south of the watershed. Areas with higher initial NDVI exhibited higher ecological stability. In the upper part of the watershed, there are some areas that have shown overall greening or browning. The areas that have experienced greening, had low resistance and showed an improvement in ecosystem functioning in response to the drought. These areas were identified as locations with high potential for land restoration.

1. Introduction

About 45 percent of the Earth is covered with drylands (Prăvălie, 2016); regions in which precipitation is exceeded by evapotranspiration, making water scarce. These drylands are a home to more than 2.5 billion people (Reynolds et al., 2007). In addition, drylands exhibit unique and rich biodiversity and have great economic potential. A majority of the world's oil resources are located in drylands (Maestre et al., 2012). Drylands are known to be vulnerable to anthropogenic pressures and climate change. Today, agricultural expansion and intensification is threatening dryland ecosystems (UNCCD, 2017). The ongoing cultivation of drylands and the transition from pastoral to sedentary lifestyles enhances desertification (Millennium Ecosystem Assessment, 2005). The increase in extreme weather events, such as droughts and heavy precipitation (IPCC, 2018) will worsen water scarcity and reduce ecosystem productivity of drylands (UNCCD, 2017). Currently, between 10 to 20 percent of global drylands are already degraded (Millennium Ecosystem Assessment, 2005). This is a human tragedy, as people that live in drylands are often reliant on its ecosystem services and have limited possibilities to seek alternative sources of income (Millennium Ecosystem Assessment, 2005; UNCCD, 2017). Land degradation threatens the livelihood of those people by compromising food security and water availability and exacerbating socio-political instability, conflicts and migration (UNCCD, 2017).

Healthy ecosystems are more resilient to the pressures exerted by humans and climate change. Holling (1973) formulated the definition of ecological resilience as the ability of a system to persist when faced with changes in system parameters and to absorb such disturbances. In ecosystems where resilience is low, a catastrophic shift may occur when a certain critical threshold is reached (Scheffer et al., 2001). When this happens an ecosystem can shift from one stable state to another: for instance from a vegetated stable state to a barren stable state. Rather than a single identifiable threshold that determines whether a degradation shift or restoration shift happens, a transitional regime exists that captures the environmental conditions under which such a shift may occur (Sietz et al., 2017). In the transitional regime, minor disturbances can cause a shift in the state of the ecosystem. In drylands, where resilience is often undermined by harsh climatic conditions and overgrazing, this poses a risk. When the system has shifted from a vegetated to a barren state, it is difficult to restore the system to its previous state. Simply returning to the conditions that existed before the catastrophic shift will not be enough: this phenomenon is called hysteresis (Scheffer et al., 2001). However, the transitional regime also presents a "window of opportunity" (Sietz et al., 2017). When environmental conditions improve, for instance due to a period of prolonged heavy precipitation (such as an El Niño episode), a degraded ecosystem may move to the transitional regime (Holmgren and Scheffer, 2001; Sietz et al., 2017). When this happens there is large potential for restoration actions, as a small intervention may push the ecosystem towards its alternative, vegetated, state. In conclusion, understanding ecosystem resilience is key in the restoration of degraded land and the prevention of catastrophic shifts that lead to degradation.

Holling's definition of ecological resilience is widely used in policy literature (Donohue et al., 2016) and literature regarding catastrophic shifts (Scheffer et al., 2015, 2001; Scheffer and Carpenter, 2003). Ecological resilience is a broad concept that encapsulates more than one dimension of ecosystem functioning in response to a disturbance. However, it does not capture the totality of metrics that describe ecosystem dynamics and its responses to disturbances. For this, the term ecological stability is used (Donohue et al., 2016; Grimm and Wissel, 1997; Kéfi et al., 2019). There are various dimensions to ecological stability. Grimm and Wissel (1997) identified constancy ("staying essentially unchanged"), resilience ("returning to the reference state (or dynamic) after a temporary disturbance") and persistence ("persistence through time of an ecological system") as the most important dimensions of ecological stability. In their assessment of ecological stability, Donohue et al. (2016) used asymptotic stability ("binary measure describing whether a system returns asymptotically to its equilibrium following small disturbances away from it"), variability ("variation of a variable over time and space") and resistance ("dimensionless ratio of some system variable measured after, compared to before, some perturbation") in addition to resilience and persistence. Many more indicators have been proposed to quantify ecological stability (Grimm and Wissel, 1997). In this context, the term resilience is used to refer to the rate at which an ecosystem returns to equilibrium after a disturbance. Holling (1996) called this "engineering resilience", however it may also simply be referred to as the recovery rate (Nes and Scheffer, 2007). In this thesis, the term ecological resilience is used for Holling's resilience and recovery rate is used for the rate at which the ecosystem moves towards equilibrium after a disturbance.

Several methods have been developed to quantify components of ecological stability. Many of these use conceptual modelling approaches to determine recovery rate or measure it after experimental perturbations (Scheffer et al., 2015). Recently, methods have emerged that make use of time-series of satellite imagery to determine the recovery rate after stochastic disturbances (Nes and Scheffer, 2007). Ponce Campos et al. (2013) studied Moderate Resolution Imaging Spectroradiometer (MODIS) satellite observations of Enhanced Vegetation Index (EVI) and quantified ecological resilience as the change in water-use efficiency (WUE) in response to drought. Von Keyserlingk et al. (2021) determined the ecological resilience of a Mediterranean dryland using Normalized Difference Vegetation Index (NDVI) satellite data. Their operationalization of the resilience concept consists of the resistance to climatic disturbances and recovery rate after a climatic disturbance as was proposed by Hodgson et al. (2015). They determined the recovery rate after a drought and resistance was quantified using the inverse of the number of breakpoints in the NDVI time-series. A breakpoint is a point in the time-series of a pixel where the trend changes significantly in magnitude and/or direction. In this study by von Keyserlingk et al. (2021) the breakpoints and recovery rate were determined using a newly developed R package: "resInd". The software uses the Breaks for Additive Seasonal and Trend (BFAST) method for change detection and registers the number of breakpoints during a time-series as well as the recovery rate after drought. The BFAST method separates seasonal, trend and noise components and distinguishes abrupt change from gradual change in a time-series with seasonality (Verbesselt et al., 2010a). Watts and Laffan (2014) assessed that the use of the BFAST method to detect abrupt change in drylands, where vegetation cover is typically only weakly impacted by seasonality, is effective. Furthermore, they demonstrated that the BFAST method can be used to detect breakpoints in response to a flooding event in a semi-arid region. De Jong et al. (2013) were the first to classify breakpoints according to the trend before and after the breakpoint. This typology was expanded and improved by Bernardino et al. (2020) in their assessment of major breakpoints in global drylands. Rather than focusing on the concept of ecological resilience, they used the breakpoint typology to quantify ecosystem functioning following Jax (2005): "a state or trajectory of a system that accounts for the totality of complex interactions occurring inside it and caused by internal or external drivers" (Bernardino et al., 2020). This is concept similar to that of ecological stability.

In this research the BFAST methodology is applied to a time-series of NDVI Landsat satellite images in the dryland ecosystem of the Ounila watershed in the High Atlas Mountains of Morocco, covering a period between 1984 and 2019. The aim of the study is to map ecological stability in the Ounila watershed. NDVI is used as an indicator of ecosystem functioning and breakpoints are considered abrupt changes in ecosystem functioning. An improvement of the breakpoint typologies of Bernardino et al. (2020) is proposed that (i) takes into account the statistical significance of the trends before and after the breakpoint, and (ii) subdivides the breakpoint typologies into positive and negative categories depending on whether they represent an improvement or deterioration of ecosystem functioning, respectively. To this end, the "resIndSpatial" function from the "resInd" package developed by von Keyserlingk et al. (2021) is expanded to register the timing and typology of breakpoints. The ecological stability of the watershed is measured by (i) the resistance of the ecosystem to abrupt changes in ecosystem functioning that lead to a deterioration in ecosystem functioning, and (ii) the ecosystem response after climatic disturbances. Climatic disturbances are defined as anomalies in precipitation: pro-longed droughts or heavy precipitation events. Resistance is determined by the inverse number of negative breakpoints. A number of negative breakpoints that is equal to or lower than the median number of negative breakpoints in the watershed, indicates relatively high resistance. The suitability of total number of breakpoints, total number of positive breakpoints and total number of negative breakpoints as an indicator for resistance is evaluated. The hypothesis that a lower number of negative breakpoints may be correlated with a higher number of positive breakpoints is tested. The ecosystem response to climatic disturbances is assessed by the occurrence of different breakpoints typologies that represent a deterioration or improvement in ecosystem functioning. Resistance and ecosystem response to climatic disturbances in the Ounila watershed are further explored by comparing them to overall change in NDVI during the monitoring period, the spatial distribution of land use classes, initial NDVI and NDVI before the occurrence of a breakpoint.

The main question answered in this study is:

What are the hotspots of (high and low) ecological stability in the face of climatic disturbances in the Ounila watershed?

To this end, the following sub-questions are formulated:

1. How has ecosystem functioning changed between 1984 and 2019 in the Ounila watershed?
2. When have major climatic disturbances taken place in the Ounila watershed between 1984 and 2019?
3. How resistant was the ecosystem of the Ounila watershed to abrupt changes in ecosystem functioning between 1984 and 2019 ?
4. How has the ecosystem responded to climatic disturbances in the Ounila watershed between 1984 and 2019?

This research is innovative since an improved typology of breakpoints is developed and applied. New indicators for recovery and resistance, that represent changes in ecosystem functioning, are tested. Furthermore, the application of the BFAST methodology and characterization of breakpoints on a dataset with such a high spatial and temporal resolution is unprecedented.

This MSc thesis is part of a larger research project that is conducted in partnership with PermaAtlas, a Dutch Moroccan NGO that is implementing restoration measures in the village of Douar Anguelz Ounila (upper east of the Ounila watershed). The aim of this larger research is to map the social-ecological networks in the Ounila watershed in order to generate knowledge that contributes to designing a sustainable food system for the region. This MSc Thesis will contribute scientific information to both the larger research project and the activities of PermaAtlas by characterising changes in ecosystem functioning between 1984 and 2019 and identifying regions of high and low ecosystem stability. The latter of particular interest for PermaAtlas to prioritise areas for restoration.

2. Case study area

The study area is the Ounila watershed (Figure 1), which is located in Ouarzazate province and encompasses an area of ~730 km^2. The watershed is enclosed by the peaks of the High Atlas Mountains in the north and stretches until the village Aït-Ben-Haddou in the south. The Asif Ounila (eastern river channel) and Asif Mellah (upper western river channel) rivers run through the watershed.

Traditionally, people in the High Atlas lived a pastoral lifestyle. In winter, the herds would reside in the lower-lying areas and in spring the herds were moved to pastures uphill (El Aich, 2018). During the summer, when rain is scarcer and temperatures are higher, larger distances are covered in search for water and vegetation. The distance travelled with the herd also depended on the size of it, as with more animals the lands are depleted sooner. The movements of the herds were managed by the so-called *Agdal* system, in which decisions were made collectively. In the area surrounding Anguelz, regulations were put in place in 1956, dividing the pastures between the shepherds. The local grazing committee, communicated and monitored these rules for livestock and grazing (Nieboer, 2019). In conclusion, the practices in the case study area were well adapted to the availability of natural resources and the seasonal variability of pastures.

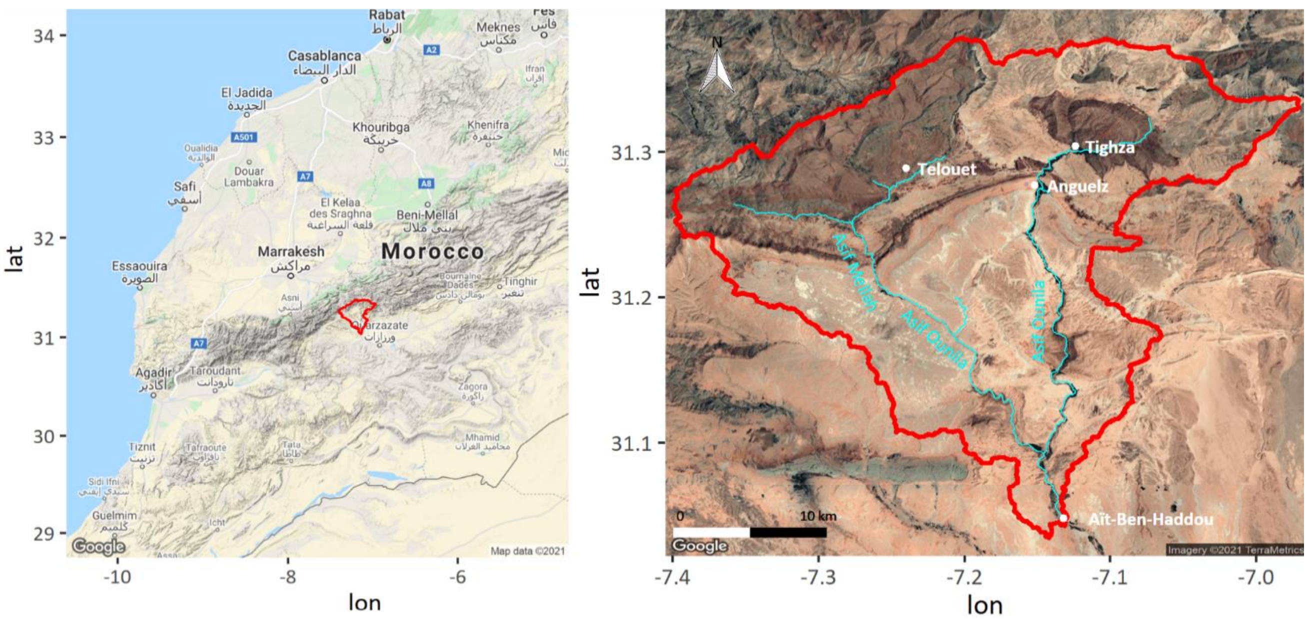

FIGURE 1 | LEFT: GOOGLE TERRAIN MAP OF MOROCCO, WITH THE CASE STUDY AREA OUTLINED IN RED. RIGHT: GOOGLE SATTELITE IMAGE OF THE CASE STUDY AREA, WITH THE LOCATION OF THE SETTLEMENTS DOUAR ANGUELZ OUNILA (ANGUELZ), TELOUET, TIGHZA AND AÏT-BEN-HADDOU AS WELL AS THE RIVER CHANNELS (ASIF MELLAH AND ASIF OUNILA) INDICATED.

However, over the past 60 years, many changes have occurred in the High Atlas Mountains. Tribes have largely abandoned their pastoralist lifestyle and have become sedentary. In general, there has been a shift towards agro-pastoralism in the Atlas Mountains, where more terraced and irrigated agriculture is practiced than before (El Aich, 2018). Due to this sedentary lifestyle the pressure on lands nearby settlements is increased and less healthy pastures are available. With motorization, outlying areas have become more accessible and the herds have therefore moved further away. On the other hand, motorization enables the transportation of water and feed to the herd, making it unnecessary to move the herd towards new pastures and sources of water. At the same time, the way the pastures are managed has drastically changed. The *Agdal* has lost its power and decisions are now more commonly made by individuals according to their financial and social status (El Aich, 2018). As a consequence of the developments of the past decades, the mobility of herds has decreased. This has stimulated overgrazing and diminished the capacity of pastures to feed the herd (El Aich, 2018; Nieboer, 2019). The shepherd of Anguelz are driven to pastures further away (> 200 km) (Nieboer, 2019).

Benassi (2008) found that between 1971 and 2000 the average amount of rainfall in Morocco has decreased by 15% compared to the rainfall in the period between 1961 and 1990. Furthermore, heavy rainfall events and droughts have increased in magnitude and frequency during this period (Benassi, 2008). In November 2014 and January 2015 heavy precipitation caused flooding in the Ounila watershed (Radiant Design Sarl, n.d.). Anguelz has a temperate climate with dry and hot summer, according to the Köppen-Geiger classification published by Beck et al. (2018) (Figure 2). The lower-lying area has an arid climate, and uphill from Anguelz, the climate is temperate, followed by a cold climate higher up the mountains, both with a dry and warm summer (see Appendix A, Figure 16 for an elevation map of the area).

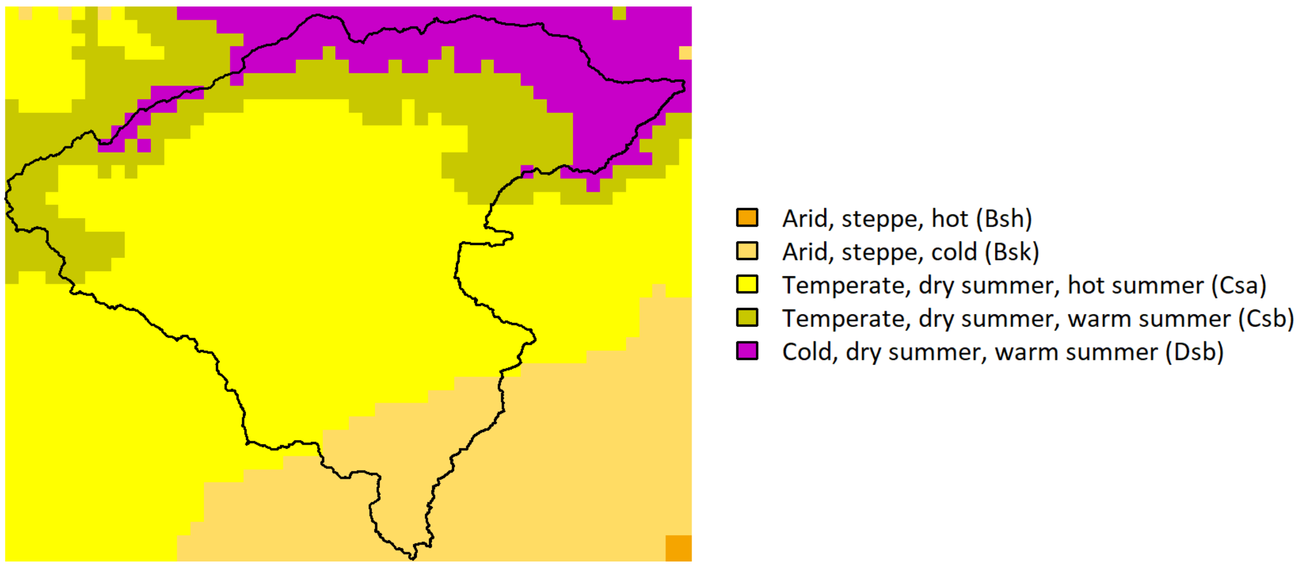

FIGURE 2 | PRESENT DAY (1980-2016) KÖPPEN-GEIGER CLIMATE CLASSIFICATION OF THE CASE STUDY AREA AT A 0.0083° RESOLUTION AS PRESENTED BY (BECK ET AL., 2018).

Figure 3 shows the land cover classification map of the Ounila watershed (European Space Agency, 2017). The major land use categories in the area are bare soil (42.5%), grassland (34.8%) and lichen mosses and sparse vegetation (19.7%). 2.5% of the land is classified as cropland. The bare areas are mainly located in the south of the watershed whereas the grasslands and sparsely vegetated areas are more dominant in the north. Cropland is located along the river channels, especially the Asif Ounila channel. In the north-west of the watershed there are also some croplands with built up areas. The higher parts of the Ounila watershed are more densely vegetated.

According to Nieboer (2019) the most common perennial species in the case study area are: *Atractylis cancellata, Bromus rubens, Launaea nudicaulis, Medicago sp and Paronychia argentea,* which are species of shrubs, grasses and herbs. Agricultural crops grown on the river banks surrounding Anguelz are "mostly Mediterranean fruit trees, legumes, and vegetables, a bit of barley, maize and animal forage to provide the basis for human and animal nutrition for the village" (Nieboer, 2019). The degraded soils in the area cannot retain the heavy rainfall well and therefore there is a lot of water runoff, causing further soil erosion, and occasionally landslides (Nieboer, 2019). A lack of water retainment makes the vegetation more vulnerable to droughts.

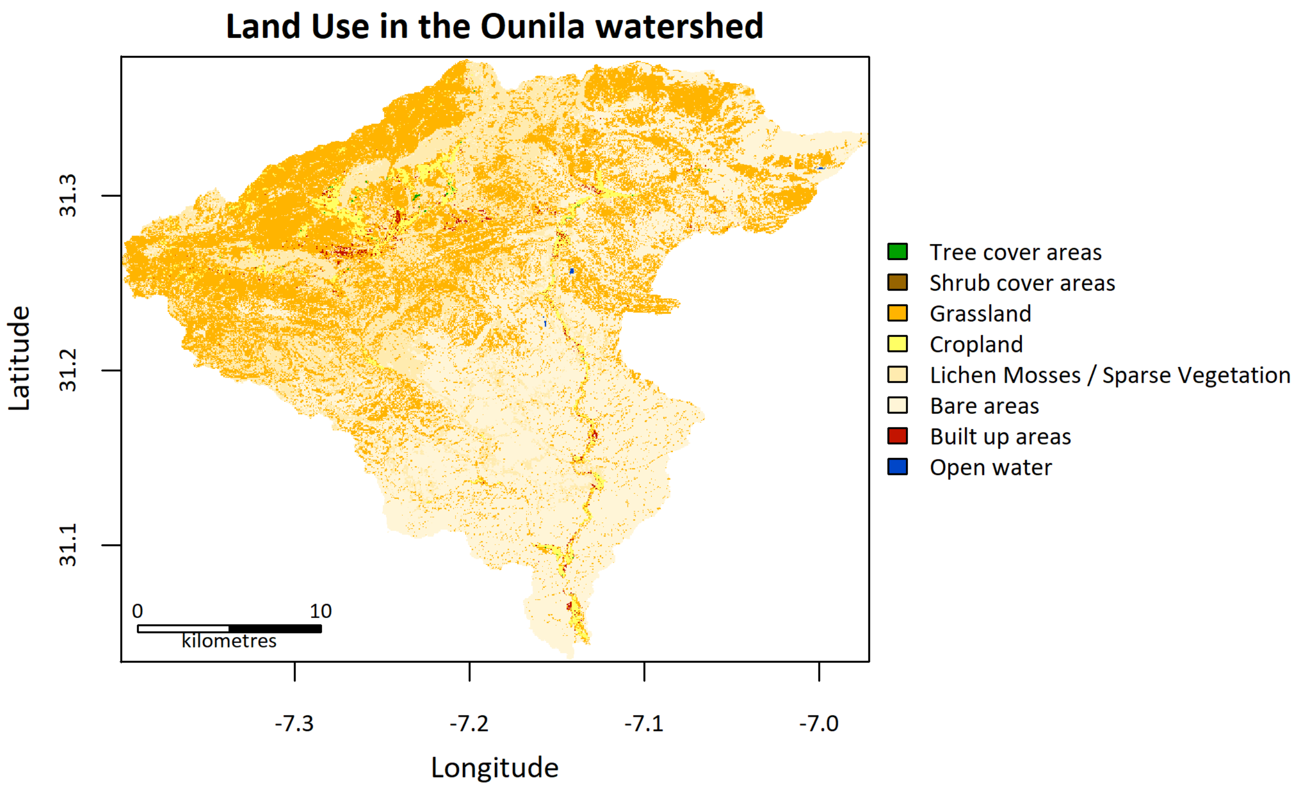

FIGURE 3 | LAND COVER CLASSIFICATION MAP (EUROPEAN SPACE AGENCY, 2017) THE CASE STUDY AREA IN 2016 AT A 20 BY 20 M SPATIAL RESOLUTION.

3. Methods

3.1. Datasets

3.1.2. NDVI

As a proxy for vegetation density and ecosystem functioning in the case study area, Normalized Difference Vegetation Index (NDVI) data from Landsat satellite imagery was used. NDVI represents the greenness and fraction of energy absorbed by the vegetation and is a function of near infrared (NIR) and red (R) energy:

NDVI = (NIR-R)/(NIR+R)

The surface reflectance NDVI product that was used is available via the EROS Science Processing Architecture (ESPA) from the archive of the U. S. Geological Survey (USGS), on demand (USGS/EROS, 2020). This data is the output of the Landsat Ecosystem Disturbance Adaptive Processing System (LEDAPS) (USGS/EROS, 2019). The total NDVI data set that was obtained covers a time period from March 1984 to December 2019. This includes images from Landsat 5 TM (March 1984 – November 2011), Landsat 7 ETM+ (July 1999 – December 2019) and Landsat 8 OLI (March 2013 – December 2019). The Landsat NDVI data has a spatial resolution of 30 m by 30 m. Landsat 5, 7 and 8 images all have a 16-daily temporal resolution. However, in the NDVI dataset that was used in this research there are images missing in between and there is a temporal overlap in the availability of NDVI products from different Landsat satellites. The result is an irregular NDVI time-series. In addition to the NDVI-product, level-1 quality flag data was acquired from the ESPA interface. The Ounila watershed covers 4 tiles with WRS-II Path/Row: 201/038, 201/039, 202/038 and 202/039. With the maximum amount of cloud cover allowed set at 100%, a total of 3492 images were obtained, corresponding to 1967 scenes on different dates.

3.1.2. Precipitation

To analyse precipitation in the area and identify climatic disturbances, ERA-5 reanalysis daily precipitation data, which has a spatial resolution of 0.1°x0.1° (native ~9km) and is accumulated to a daily temporal resolution (Copernicus, 2020) was used. In order to have a good coverage of the Ounila watershed, this data was reprojected to the same resolution as the NDVI data. The ERA-5 Reanalysis data currently has the highest spatial and temporal resolution of all freely available precipitation data. Reanalysis data are a combination of field observations and output from atmospheric circulation models, these are used to inform a continuous spatiotemporal dataset. Typically, the product is closer to model output than observational data in remote areas, where it is likely that fewer ground observations have informed the reanalysis.

3.1.3. Ancillary data: DEM and land use data

The NASA Making Earth System Data Records for Use in Research Environments (MeaSUREs) Digital Elevation Model (DEM) dataset (Buckley et al., 2020) was downloaded via the NASA EOSDIS Land Processes Distributed Active Archive Center (LP DAAC) Data Pool (LP DAAC, n.d.). The data has a spatial resolution of 30 by 30 m and was acquired in HGT format Using the raster package. The NASADEM data was converted to GeoTIFF format and reprojected to geographic (WGS84) projection. The product contains a pre-calculated slope (°) product that was used as ancillary data. The aspect (°) was calculated from the DEM data. The land use product that was used is a prototype land use map of the African continent for the year 2016 on a spatial scale of 20 by 20 m (European Space Agency, 2017).

3.2. Determination of climatic disturbances

The Standardized Precipitation Index (SPI) (McKee et al., 1993) was used to determine the occurrence and duration of droughts. The SPI is best determined on a time-series of at least 30 years, making it a very suitable indicator to apply on the NDVI time-series studied in this research. Calculation of the SPI requires that the precipitation data is normally distributed. In order to meet this requirement, a cube root transformation was applied to the precipitation data. The SPI was calculated per hydrological year, which runs from October until September following the definition of the U.S. Geological Survey (n.d.), using a yearly averaging period. According to the definition by McKee et al. (1993) a drought period starts when the SPI reaches -1 and is over when the SPI is above 0 again. The different drought categories, as formulated by McKee et al. (1993) are shown in Table 1.

SPI value	Drought Category
0 to -0.99	Mild drought
-1.00 to -1.49	Moderate drought
-1.50 to -1.99	Severe drought
≤ -2.00	Extreme drought

TABLE 1 | DROUGHT CLASSES RELATED TO SPI FOLLOWING MCKEE ET AL. (1993)

The duration of the flooding period was determined by calculating the Rainfall Anomaly Index. For this, the "rai" function of the R package "precintcon" was used (Povoa and Nery, 2016). This function uses the method developed by van Rooy (1965) to calculate rainfall anomaly. The function arranges the precipitation data in descending order. The mean of the highest ten and lowest ten values are calculated for an averaging period of one year and set as a threshold for the positive and negative Rainfall Anomaly Index, respectively.

3.3. Detection and classification of abrupt changes in ecosystem functioning

3.3.1. Pre-processing of the satellite data

For each of the 1967 dates there were between one and 4 tiles with NDVI data. All pixels with a value of -9999 (fill value) and 20000 (saturated pixels) were set to NA before mosaicking the tiles together. The mosaicked scenes were then sorted in chronological order. The quality flag data was processed in similar steps, with the difference that in this product there were no saturated or filled pixels removed. Using the quality flag, all clouds, snow, ice, water and clouds shadows were masked out of the data, leaving pixels with NA. A scaling factor (0.0001) was then applied to scale the NDVI data to values between -1 and 1. Pixels with negative values were removed as the NDVI of natural vegetation over land is above zero. Subsequently the data was reprojected to geographic (WGS84) projection and masked to the extent of the Ounila watershed.

After elimination of the low quality and cloud covered pixels there were some scenes that did not contain data. Those scenes were removed. In addition, there were some scenes with erroneous data due to sensor failures, especially in the later Landsat 5 images. This is most likely due to old mirror bumpers, causing synchronization failures between the shutter and primary scan mirror. After removing these scenes, 1834 scenes remained. In Figure 19 of Appendix B, an overview of the number of scenes over time is given. On 31 May 2003, the Scan Line Corrector (SLC) of Landsat 7 failed, resulting in data gaps from this date onwards. In the Level-2 NDVI product, all these errors are already masked out. The SLC failure did not have a large impact on the spatial distribution of NA frequency in the Ounila watershed (see Figure 20, Appendix B).

Finally, due to a difference in spectral response functions of the ETM sensor of Landsat 4-7 and the OLI sensor of Landsat 8 the NDVI data were not continuous: there was an offset between the data from different sensors (see Figure 21, Appendix C). Therefore, the Landsat 5-7 images were transformed using the following linear relationship proposed by Roy et al. (2016) for NDVI surface reflectance data:

OLI = 0.0235 + 0.9723 * ETM+

3.3.2. The breakpoints detection procedure

The first step in the breakpoint detection procedure is to test whether there is a significant deviation from structural stability. When a breakpoint occurs this means that there is an abrupt change in mean response. In this study, mean response was modelled by:

```
response ~ (trend + harmon)
```

In this form of the General Linear Model (GLM) there is an intercept, a trend, and between one and three harmonic components, depending on the value chosen for the order. The harmonic component consists of a sinus and cosinus component. MOSUM OLS method was used to test the null hypothesis that the regression coefficients do not change over time. If the test is significant that means that at least one breakpoint can be detected.

In case the structural stability test was significant, the “breakpoints” function from the “strucchange” package was used to find an optimal model fit and determine the number and dates of breakpoints. The goodness of fit is assessed by the Bayesian Information Criterion, which includes a penalty for the inclusion of more breakpoints to avoid overfitting (Zeileis et al., 2002).

After the breakpoints were identified a GLM was fitted to the segments between the breakpoints:

```
formula = response ~ segment/(trend + harmon)
```

A robust linear regression method using iterated re-weighted lest squares (IWLS) was used. This form of regression is particularly useful in case there are outliers present in the data. This is the case in for the NDVI data, despite the removal of erroneous scenes and low-quality pixels. To confirm that IWLS regression indeed resulted in a better fit to the data than OLS regression, the relative effectiveness of each model was calculated for a few example pixels.

3.3.3. The typology of breakpoints

The “resInd” package developed by von Keyserlingk et al. (2021) was expanded to classify breakpoints based on the trend before and after the breakpoint. To this end a new typology was developed, shown in Figure 4. There are nine type of breakpoint categories, based on the sign and significance of the slopes before and after the breakpoint.

The typology is based on the typology proposed by Bernardino et al. (2020). In their typology Bernardino et al. (2020) only considered significance relevant in the case of positive reversal and negative reversal. The reversal was deemed complete when both slopes are significant and incomplete when one of the slopes (either before or after the breakpoint) was not significant. In the typology proposed in this research, significance of slopes was included in all breakpoint typologies. The significance was determined based on (95%) confidence intervals around the trend. A distinction was made between breakpoints that show a more positive trend after the breakpoint compared to before the breakpoint and breakpoints that show a degrading trend compared to the trend pre-breakpoint. In other words: positive breakpoints (“interrupted increase”, ”increase after no trend”, ”no trend after decrease”, ”positive reversal”) and negative breakpoints (“interrupted decrease”, ”decrease after no trend” ,”no trend after increase”, ”negative reversal”). The positive breakpoints can be interpreted as an improvement of ecosystem functioning whereas the negative breakpoints represent a deterioration of ecosystem functioning. The “no trend after decrease”, “increase after no trend”, “no trend after increase” and “decrease after no trend” typologies correspond to the transitional state as mentioned by Bernardino et al. (2020), with the inclusion of a differentiation between a significant trend before or after the breakpoint.

Bernardino et al. (2020) included a difference between trends that are accelerating or slowing down based on the fact whether the increase/decrease is larger before or after the breakpoint. However, it was not considered whether the trends before and after the breakpoints differed significantly from each other. Furthermore, it can be argued that to conclude whether the acceleration or slowing down of a trend is actually meaningful, it would be necessary to look at the effect size of such a change in addition to significance. In the typology proposed in this research, the differentiation between a slowing down and accelerating trend is omitted. The typologies are only based on the direction and significance of the trends, and not on their relative magnitudes, this results in a manageable number of breakpoint categories that have a solid theoretical basis and practical meaning in terms of ecosystem functioning.

3.3.4. Input parameters

For the expanded "resIndSpatial" function a few input parameters had to be selected, namely the order and the h parameter. Watts and Laffan (2013) conducted a sensitivity analysis on different h values in a sparsely vegetated area and found that a value of 0.2 or smaller resulted in smaller confidence intervals around the timing of breakpoints than a value above 0.2. In the data-set of the Australian dryland that Watts and Laffan (2014) used, this h-value corresponded to +/- 3 years in between breakpoints. Following these recommendations and the manual inspection of a few example pixels in the Ounila watershed, it was found that an h value of 0.10 was best for the data in this study. This means that the minimum segment size between observations was 184 and a maximum number of 10 segments and 9 breakpoints might be fitted. This translates to an average minimum period of 3.5 years in between breakpoints. After inspection of the relative Efficiency of different values for order on a few example pixels it was determined that a value of 2 was most suitable for the NDVI data in the Ounila watershed.

3.3.6. Postprocessing of "resIndSpatial" output

Because the case study area is very large, the input NDVI data was sub-divided in smaller sub-sections. The adapted "resIndSpatial" function was subsequently executed on these smaller sub-sections. Once the output was generated the sub-sections had to be merged together. Croplands were masked out of the layers containing the indicators for ecological stability (number of breakpoints, and breakpoint types), because conclusions on ecological stability can not be drawn from data of managed and irrigated land.

3.4. Statistical analysis

To calculate the correlation between the total number of positive and negative breakpoints the Spearman correlation method was used. The correlation coefficient was calculated on a moving window of 7 by 7 (49) pixels to account for spatial variations in correlation. This window size was chosen in order to obtain a decent group size (>30) and still retain a high spatial resolution. The "rasterCorrelation" function from the R-package "spatialEco" was used for this (Evans, 2020).

3.5. Software, scripts and availability of data

All scripts that were used in this research are available via https://github.com/angeliquelv/ThesisSUSD. Most data processing and analysis was conducted using RStudio (RStudio Team, 2018). The adapted "resIndSpatial" algorithm was applied on the data with the help of a High-Performance Computing Facility. The sub-sections were submitted to nodes with 24-cores to enable parallel processing of pixels.

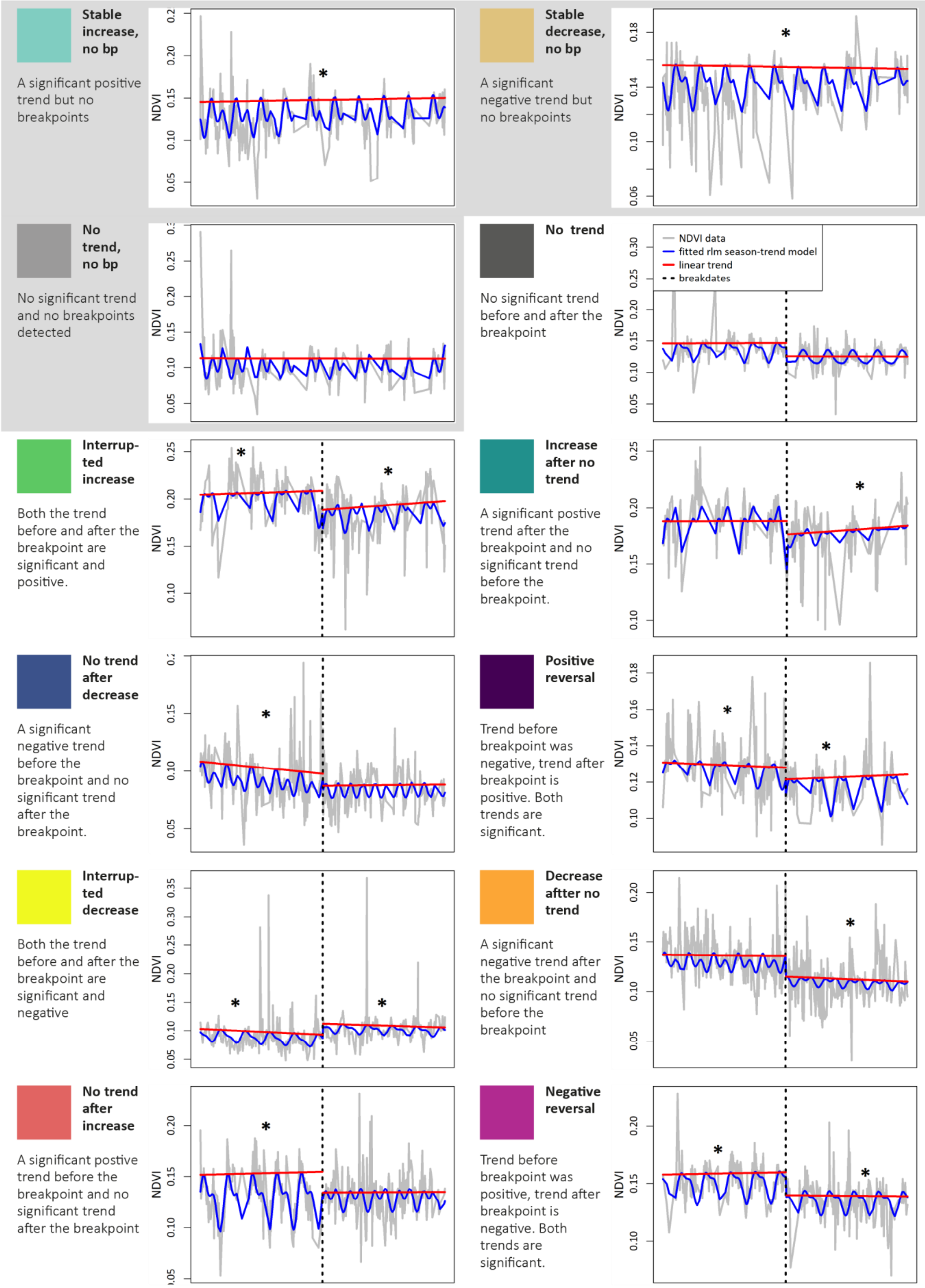

FIGURE 4 | TYPOLOGY OF TRENDS AND BREAKPOINTS. THE GREY BACKGROUND INDICATES THAT THESE TYPES HAVE NO BREAKPOINT.

4. Results

4.1. Ecosystem functioning between 1984 and 2019

Figure 5 shows that the majority of the Ounila watershed has seen no remarkable increase (greening) nor decrease (browning) in NDVI. When looking at the relative change in NDVI between 1984 and 2019, it seems like there has not been major land degradation in most of the watershed. A few patches of land show a slight decrease in NDVI. However, the absolute decrease in NDVI has been very small in all locations that experienced browning (Appendix D, Figure 22). In the upper part of the watershed there has been more change in NDVI compared to the lower part of the watershed. The NDVI during first three years of the monitoring period (1984-2019) was higher in the upper part of the watershed too (Appendix D, Figure 23). In conclusion, the areas that initially had a higher vegetation cover, also experienced a stronger increase in vegetation cover during the monitoring period. The croplands in the Asif Ounila river channel, located in the eastern part of the watershed have experienced greening. Croplands in the north-east of the watershed have experienced a strong increase in NDVI as well.

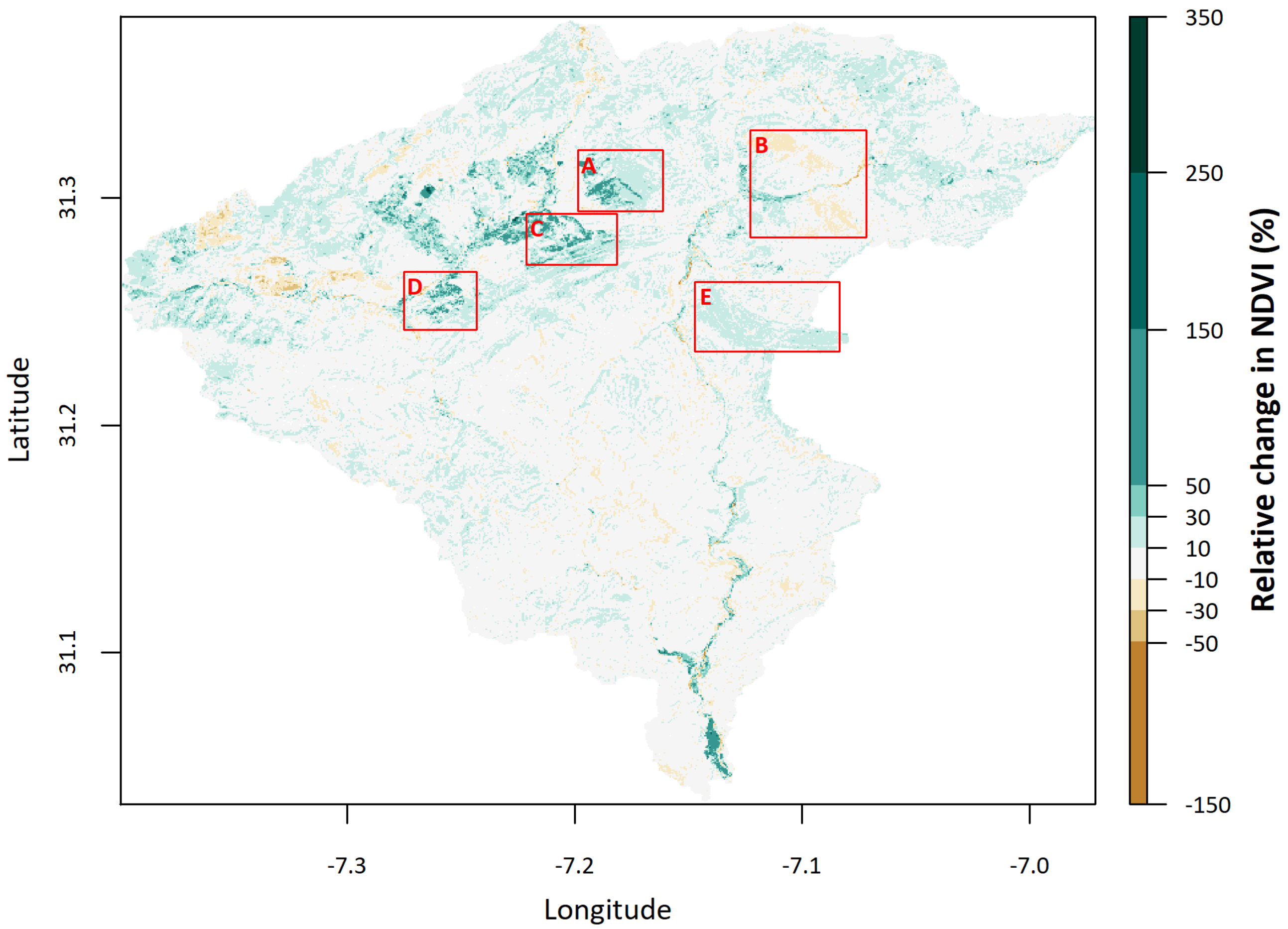

FIGURE 5 | RELATIVE CHANGE IN NDVI IN THE OUNILA WATERSHED BETWEEN THE FIRST THREE YEARS OF THE MONITORING PERIOD (1984-2019) AND THE LAST THREE YEARS OF THE MONITORING PERIOD. IN THE RED BOXES AREAS OF INTEREST ARE INDICATED. SPATIAL RESOLUTION IS 30 BY 30 M.

Five areas of interest are defined that are studied in more detail: these are indicated in Figure 5. The areas of interest are regions that have shown remarkable greening or browning. They have experienced an improvement or deterioration in ecosystem functioning, respectively. Therefore, they are potential hotspots of high and low ecological stability. Areas that contained many pixels that were classified as cropland or showed tree plantations in satellite images were not selected as areas of interest because these are most likely irrigated. In Appendix E, a map of relative change in NDVI without croplands and satellite images of the selected areas of interest are provided.

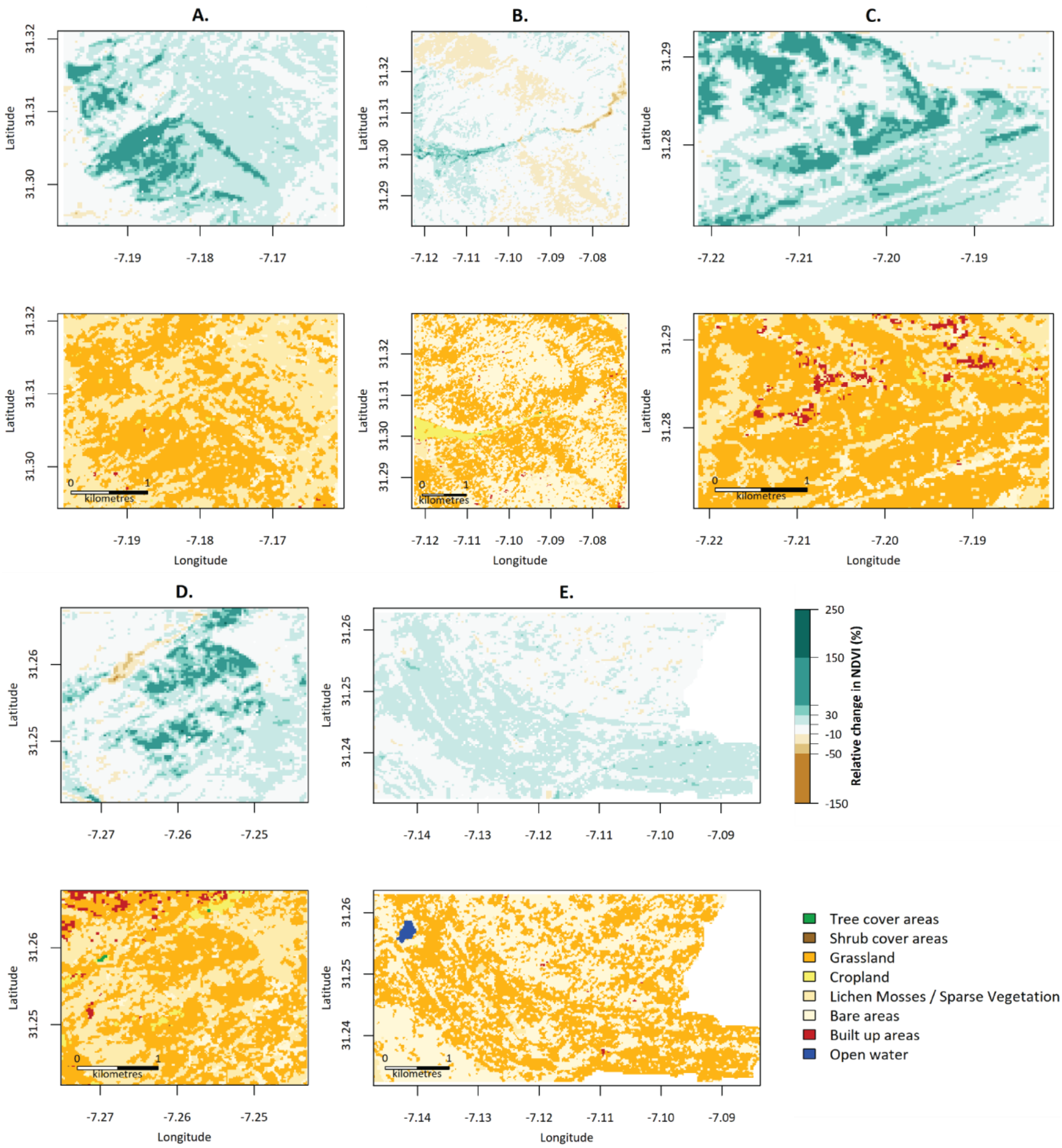

FIGURE 6 | ZOOMED IN PLOTS OF RELATIVE CHANGE IN NDVI BETWEEN FIRST AND LAST THREE YEARS OF MONITORING PERIOD (1984-2019) AND LAND USE CLASSIFICATION IN 2016 (EUROPEAN SPACE AGENCY, 2017) FOR THE AREAS OF INTEREST: A-E. SPATIAL RESOLUTION OF NDVI AND LAND USE DATA IS 30 BY 30 M AND 20 BY 20 M, RESPECTIVELY.

In Figure 6 the relative NDVI change and land use are shown for each of the areas of interest. Area A, C and D are part of a lower-lying region surrounding Telouet (see Appendix A, Figure 16) that also contains croplands and tree plantations. Area A, located east of Telouet and west of Tighza, has experienced an increase in NDVI, especially in the pixels classified as grassland. The north-facing slopes (Appendix A, Figure 18) of area C and D, located slightly south and south-west of Telouet, respectively, have also experienced greening that is more prominent in the grassland parts. Both (C and D) contain some pixels that are classified as built up areas. However, satellite images of these areas show that this is not the case (Appendix E). The land use map is thus not entirely accurate in classifying built-up areas. Area B shows the lands surrounding Tighza that experienced browning. There are much more barren pixels here than in the other areas of interest. Finally, the area that experienced a slight greening south-east of Anguelz (E) is predominantly covered with grassland. The area consists of south and north facing slopes (Appendix A, Figure 18) and the greening is mostly visible on the north-facing slopes.

Figure 7 shows that the overall NDVI in the Ounila watershed is low and not very sensitive to seasonal variation. The seasonal amplitude varies between 0.025 and 0.1 approximately. The occurrence of breakpoints over time does not seem to be heavily impacted by the number of scenes (Appendix B, Figure 19): although the number of available scenes increases over time there is no apparent increase in number of breakpoints detected over time. Rather, the number of breakpoints detected seem to correspond to the Rainfall Anomaly Index. This is especially visible between the year 2000 and 2003 and in 2015. In 2000-2002 there is an extended period of negative RAI followed by a peak in breakpoint occurrence. In the end of 2014 there is a peak in positive RAI closely followed by a peak in breakpoint occurrence. Both negative and positive extremes in RAI appear to impact the occurrence of breakpoint. This confirms the assumption that climatic disturbances, in the form of droughts as well as heavy precipitation events may induce breakpoints in the NDVI time-series.

4.2. Climatic disturbances

The SPI per hydrological year was calculated (Table 2). The drought started with a moderate drought period in 1999. In the following three years the drought developed from mild, to extreme to severe. In 2003 the SPI was positive again and the drought period ended. In conclusion, the drought period lasted from October 1998 until September 2002.

Year	SPI	Year	SPI	Year	SPI	Year	SPI	Year	SPI
1985	-0.05	1992	-0.19	1999	-1.39	2006	0.23	2013	-0.49
1986	1.21	1993	-0.81	2000	-0.49	2007	0.78	2014	-0.60
1987	0.15	1994	0.20	2001	-2.47	2008	-0.66	2015	1.27
1988	1.36	1995	-0.84	2002	-1.52	2009	1.10	2016	-0.38
1989	0.73	1996	0.55	2003	0.07	2010	-0.01	2017	0.21
1990	1.33	1997	0.49	2004	0.68	2011	0.65	2018	-0.39
1991	-0.07	1998	0.33	2005	-0.82	2012	-0.06	2019	0.27

TABLE 2 | SPI PER HYDROLOGICAL YEAR IN THE OUNILA WATERSHED. BROWN SHADING INDICATES THE YEARS IN WHICH THERE WAS A DROUGHT ACCORDING TO THE CLASSIFICATION OF (MCKEE ET AL., 1993).

To determine the flood period the Rainfall Anomaly Index per hydrological year was calculated (Appendix E, Figure 26). As is also visible in Figure 7, there is one year with a much higher positive rainfall anomaly; namely the hydrological year of 2015. This also corresponds to the incidence of heavy precipitation events in Anguelz in November 2014 and January 2015 (Radiant Design Sarl, n.d.).

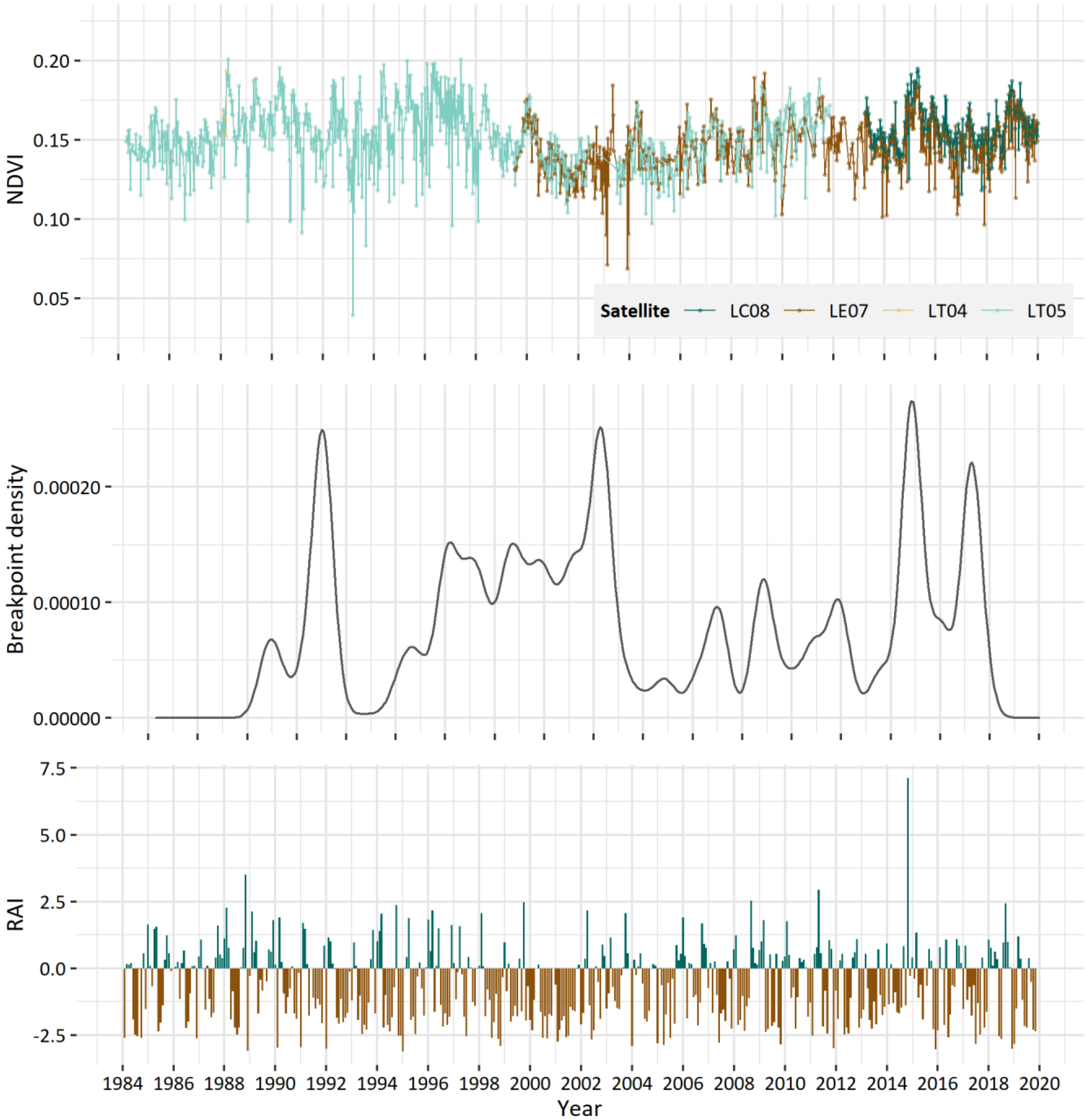

FIGURE 7 | UPPER: TIME-SERIES OF MEAN NDVI IN THE OUNILA WATERSHED BETWEEN 1984 AND 2019 WITH THE SATELLITE THAT COLLECTED THE DATA INDICATED. MIDDLE: DENSITY OF THE NUMBER OF BREAKPOINTS REGISTERED BETWEEN 1984 AND 2019. LOWER: RAINFALL ANOMALY INDEX PER MONTH BETWEEN 1984 AND 2019.

4.3. Resistance to abrupt changes in ecosystem functioning

The inverse of the negative number of breakpoints is considered a proxy for resistance. The median of the total number of negative breakpoints in the Ounila watershed is two. When the number of negative breakpoints in the watershed is between zero and two, resistance is considered to be relatively high. When the total number of negative breakpoint is above two, resistance is considered to be relatively low. In the upper part of the Ounila watershed, the total number of negative breakpoints is considerably lower than in the lower part of the watershed (see Figure 8). In the most northern part, there are even pixels that contain no negative breakpoints at all and many pixels that contain only one or two negative breakpoints, indicating that resistance is high. The region with the lowest number of negative breakpoints has the highest altitude and steepest slopes (see Appendix A, Figure 16 and Figure 17). In the centre and in the south of the watershed there are more negative breakpoints present. The most frequently occurring negative breakpoint types are interrupted decrease and negative reversal (see Appendix G, Figure 27). Areas with a high number of negative breakpoints are predominantly bare areas (see Appendix H, Figure 29). However, the location in the watershed (upper north or lower south) has a larger impact on the number of negative breakpoints than land use type. In the areas of particular interest that showed greening (Area A, C, D and E, Figure 6), the number of negative breakpoints is relatively high with most pixels having values between three and six. The number of positive breakpoints is high as well, with many pixels having values between three and five (Figure 9). Remarkably, the area surrounding Tighza (B), where browning has occurred, has a low number of negative breakpoints in many of the pixels, indicating high resistance (Figure 9 B). However, some of the pixels that showed browning, especially those in the north-west corner of the area, have three or more negative breakpoints indicating low resistance to abrupt changes in ecosystem functioning.

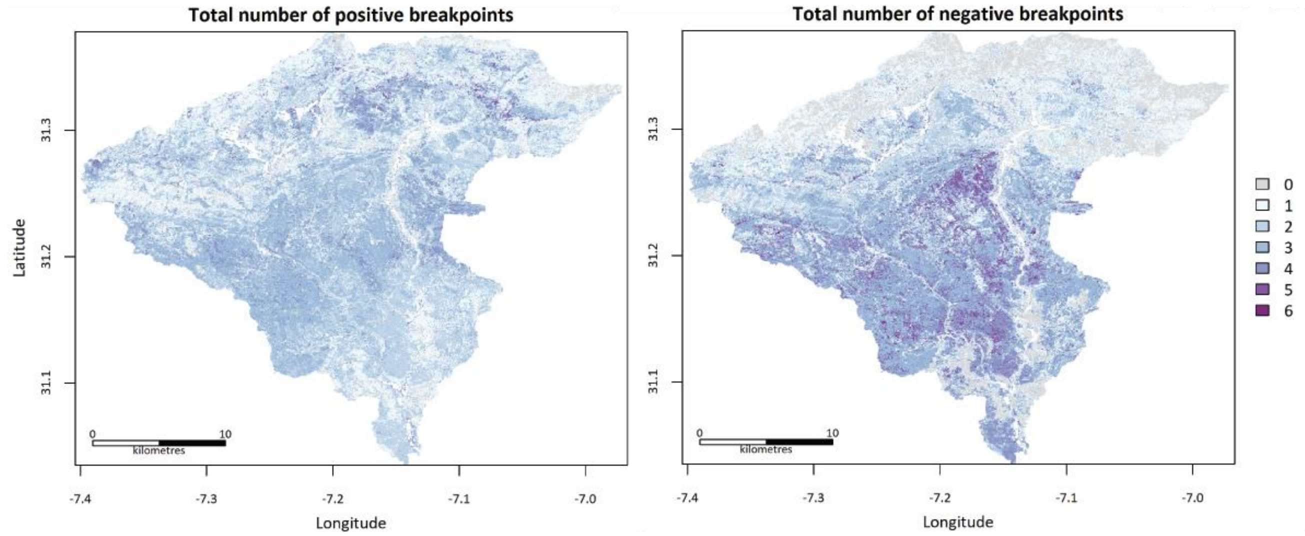

FIGURE 8 | LEFT: TOTAL NUMBER OF POSITIVE BREAKPOINTS BETWEEN 1984 AND 2019 IN THE OUNILA WATERSHED WITH CROPLANDS MASKED OUT. RIGHT: TOTAL NUMBER OF NEGATIVE BREAKPOINTS BETWEEN 1984 AND 2019 IN THE OUNILA WATERSHED WITH CROPLANDS MASKED OUT.

There is less contrast between number of positive breakpoints in the upper and lower watershed than for the number of negative breakpoints. Some hotspots of high number of positive breakpoints are located in the north. These regions of higher positive breakpoints are classified as grassland. The dominant negative breakpoint types are interrupted increase and positive reversal (see Appendix G, Figure 28). There are slightly more positive breakpoints located in the bare areas of the centre-east part of the watershed (see Appendix H, Figure 30). The total number of positive and negative breakpoints accumulated, is higher in the lower part of the Ounila watershed than the upper part (Appendix I, Figure 32). Grassland and sparse vegetation, experienced more breakpoints than bare areas (see Appendix H, Figure 31). In general, the results for the total number of breakpoints and the total number of negative breakpoints are similar.

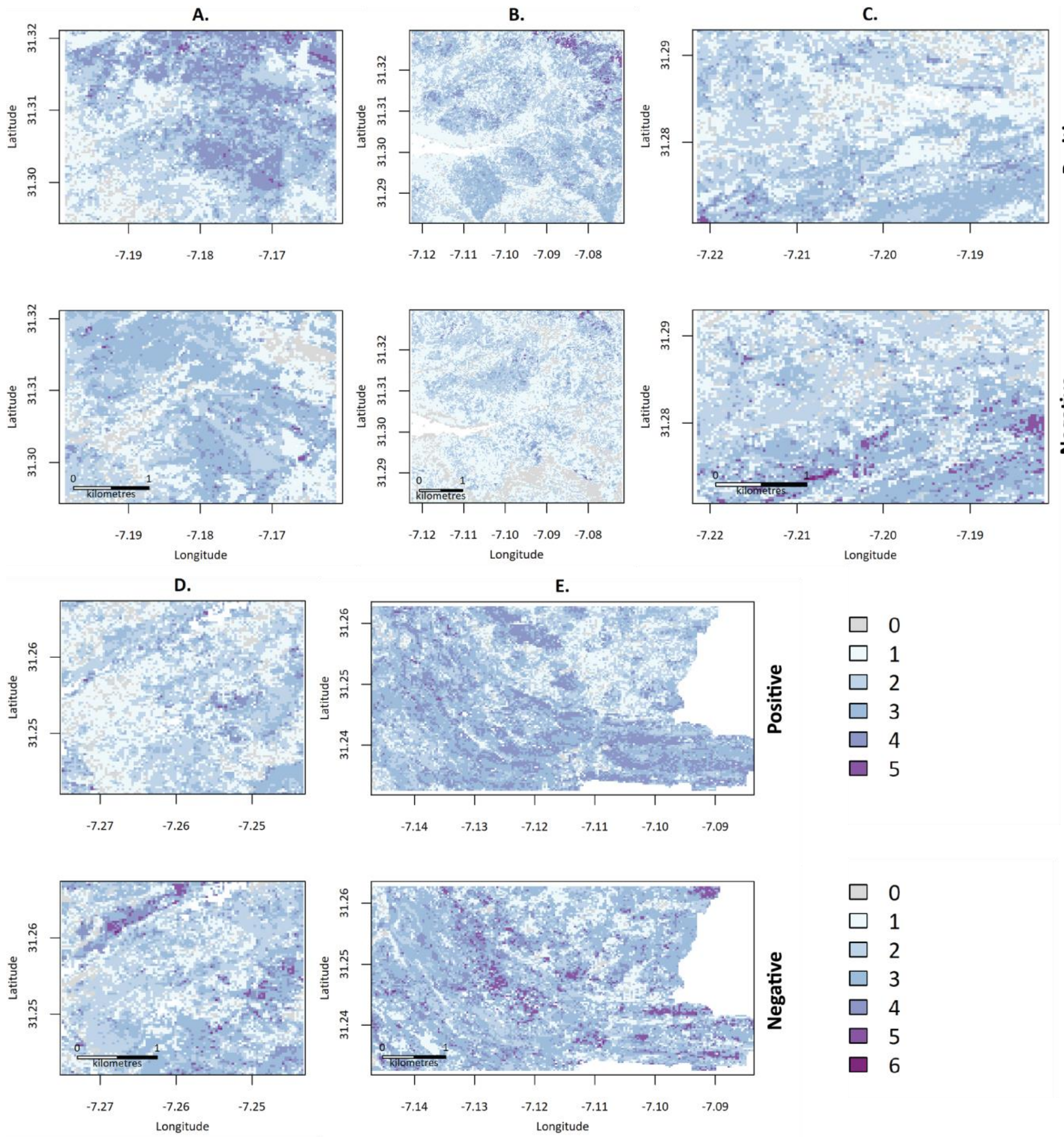

FIGURE 9 | ZOOMED IN PLOTS OF TOTAL NUMBER OF POSITIVE AND NEGATIVE BREAKPOINTS DETECTED PER PIXEL BETWEEN 1984 AND 2019 FOR THE AREAS OF INTEREST: A-E. SPATIAL RESOLUTION OF IS 30 BY 30 M

When comparing the total number of negative breakpoints with the total number of positive breakpoints in Figure 8, it stands out that in many areas where no negative breakpoints occurred, positive breakpoints did occur. Furthermore, in the areas where there were the most negative breakpoints, far less positive breakpoints were present. In Figure 10, the correlation between the total number of positive and the total number of negative breakpoints is shown. This map shows that the correlation between the two indicators varies from -1 to 1: meaning that in some locations there is a positive correlation between the two and in some places a negative. It indeed shows that a negative correlation is present in large parts of the watershed.

However, the sign of correlation between negative and positive breakpoints depends on location and seems to be more negative in areas with low vegetation cover and a high number of total breakpoints (bare areas).

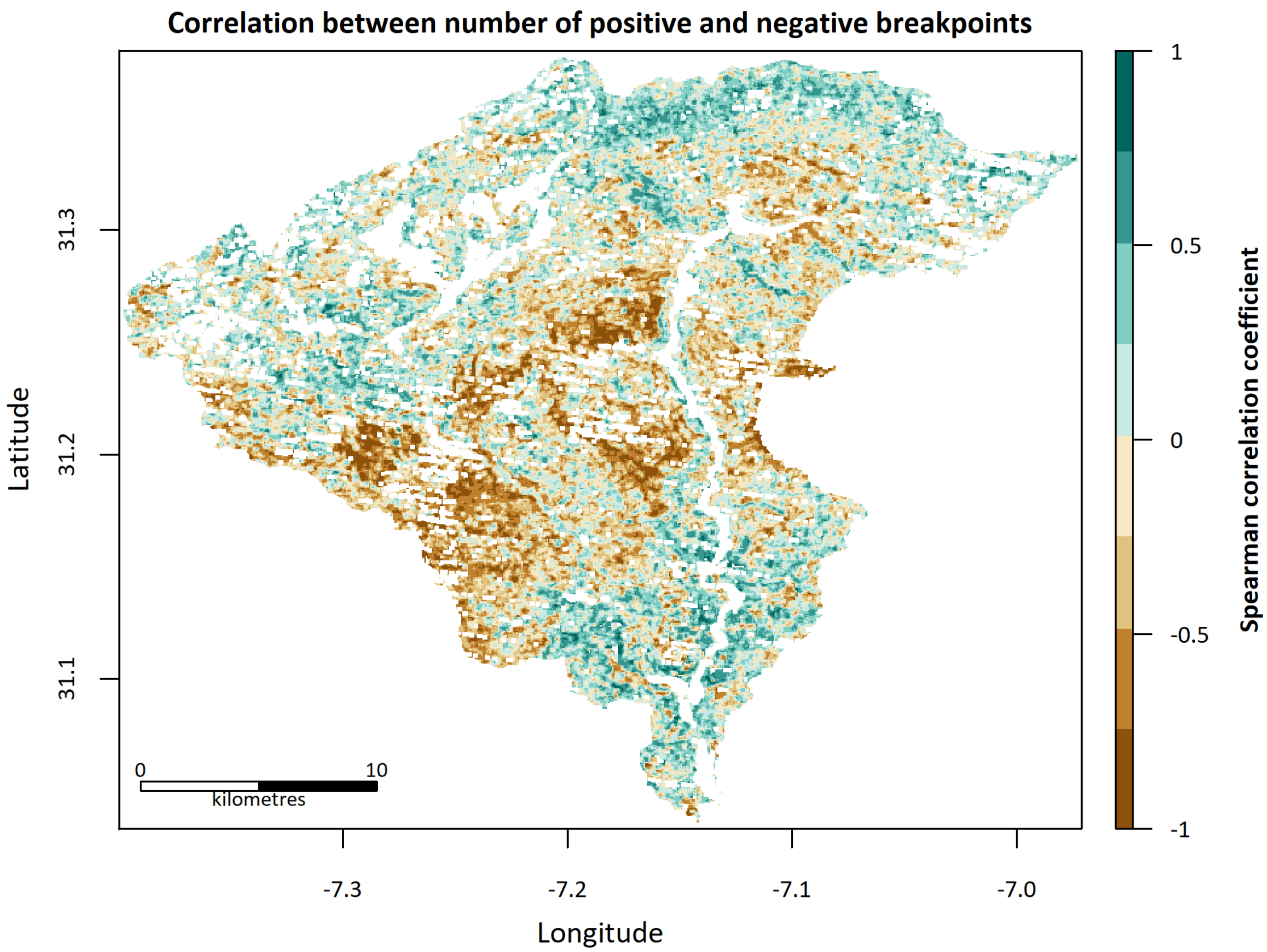

FIGURE 10 | MOVING WINDOW CORRELATION BETWEEN THE NUMBER OF NEGATIVE AND THE NUMBER OF POSITIVE BREAKPOINTS USING SPEARMAN'S CORRELATION METHOD. THE CORRELATION COEFFICIENT IS CALCULATED OVER A MOVING WINDOW OF 7 BY 7 PIXELS (N=49).

4.4. Ecosystem response after climatic disturbances

4.4.1. Ecosystem response after a drought

In the majority of the Ounila watershed (77.7%) a breakpoint occurred during the drought period in the hydrological years 1999-2002. In 1.4% of breakpoints there was no trend before or after the breakpoint, 52.0% of breakpoints were positive and 24.3% of breakpoint were negative. The dominant breakpoint type was the positive reversal. The map in Figure 11 shows that the positive reversal type was especially dominant in the upper part of the watershed, whereas in the lower part of the watershed more pixels followed an interrupted increase. In any case, this indicates that NDVI was decreasing before the drought, but after the drought areas in the upper part of the watershed, especially those covered with grassland have experienced a transition towards an increase in NDVI.

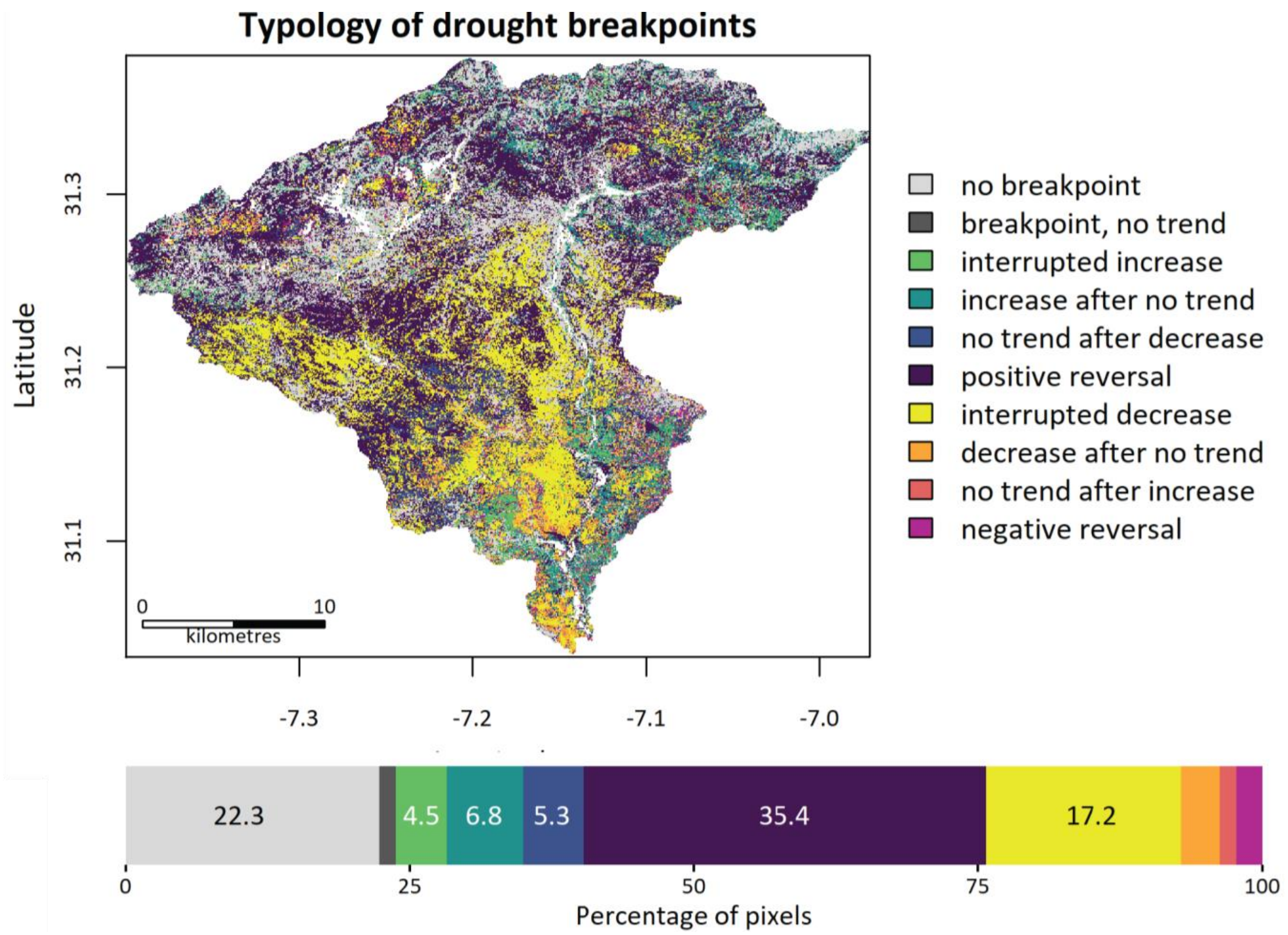

FIGURE 11 | MAP OF THE OUNILA WATERSHED WITH THE TYPOLOGY OF BREAKPOINTS THAT OCCURRED DURING THE DROUGHT PERIOD (HYDROLOGICAL YEAR 1999-2002). BELOW THE MAP: BAR WITH THE PERCENTAGE OF PIXELS THAT FOLLOW A CERTAIN TYPOLOGY.

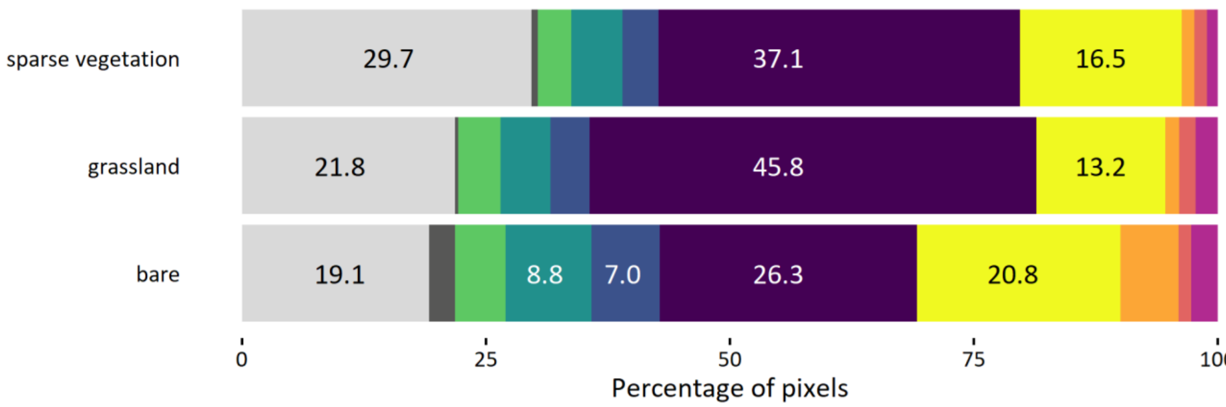

FIGURE 12 | BAR WITH THE PERCENTAGE OF PIXELS THAT FOLLOW A CERTAIN BREAKPOINT TYPOLOGY FOR EACH OF THE MAJOR LAND USE CLASSES: SPARSE VEGETATION, GRASSLAND AND BARE AREAS.

In Figure 12, the percentage of pixels that follow a certain breakpoint typology for each of the major land use classes in the Ounila watershed is shown. Bare soil has the lowest percentage of pixels with a positive breakpoint following the drought and the highest percentage of pixels with a negative breakpoint. Pixels that are classified as sparse vegetation have the highest percentage of pixels without a drought breakpoint. In the areas that are covered with grassland 45.8 percent of the pixels follow the positive reversal breakpoint typology. Areas that are more vegetated have a higher occurrence of positive breakpoints.

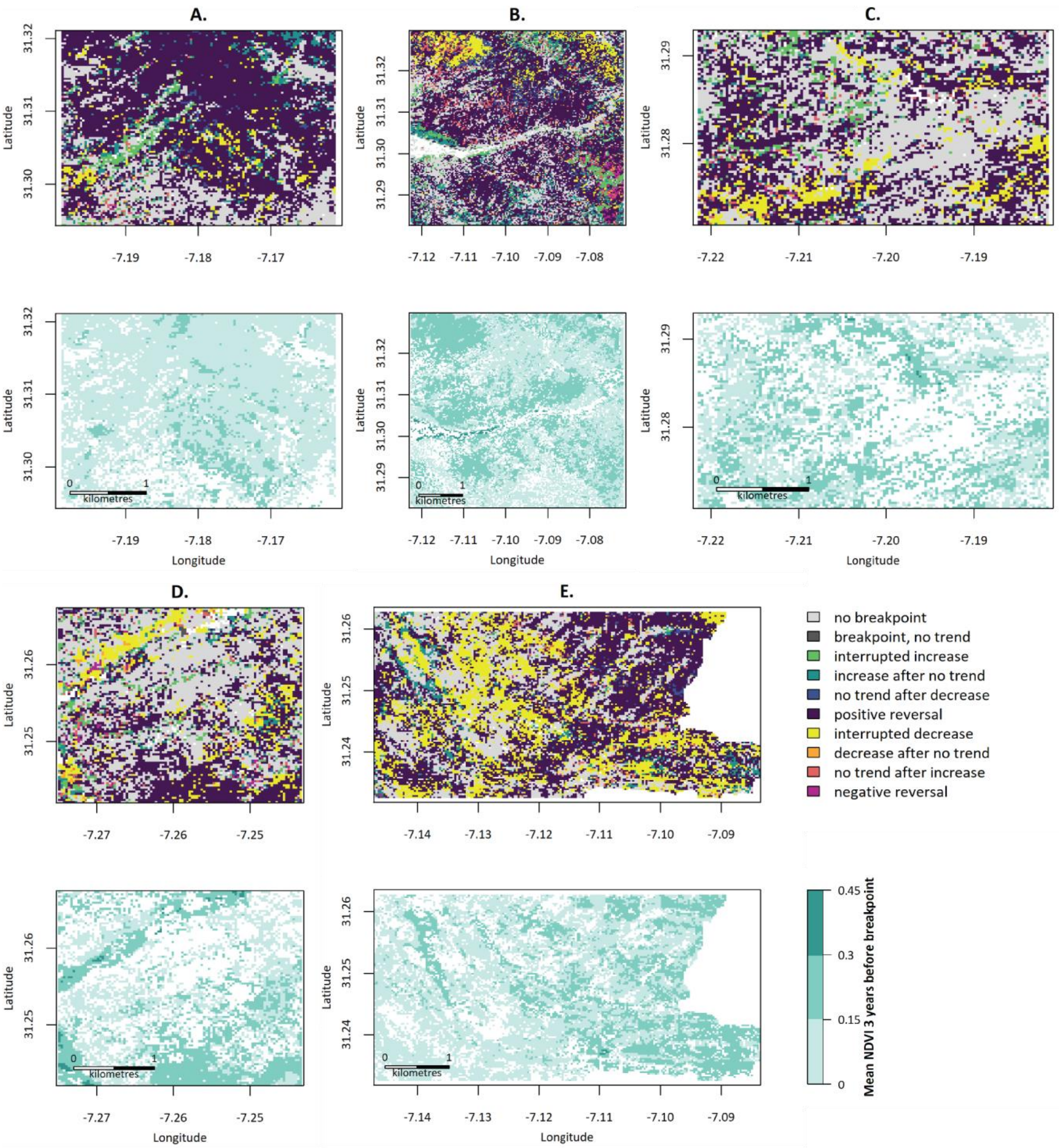

FIGURE 13 | ZOOMED IN PLOTS OF THE TYPOLOGY OF THE BREAKPOINTS DURING THE DROUGHT (HYDROLOGICAL YEAR 1999-2002) AND THE NDVI DURING THREE YEARS BEFORE THE DROUGHT BREAKPOINT FOR THE AREAS OF INTEREST: A-D. SPATIAL RESOLUTION OF BOTH DATA IS 30 BY 30 M.

Figure 13 shows the distribution of drought breakpoint types and NDVI in the three years before the drought breakpoint for each of the areas of interest. In area A and B the dominant drought breakpoint type is the positive reversal. What stands out is that some pixels that showed browning near Tighza (Figure 6, area B), have experienced an interrupted decrease (north-west of area B), whereas some are classified as positive reversal. The pixels with interrupted decrease type had relatively high NDVI before the drought breakpoint. In area C and D, relatively high number of pixels experienced no abrupt change in ecosytem functioning during the drought. In area D, the pixels that showed browning (see Figure 6) experienced an interrupted decrease during the drought. In area E, the greened land south-east of Anguelz, there are many pixels with interrupted decrease and positive reversal typologies. Here, the areas that had a higher NDVI before the breakpoint, seem to have a higher occurrence of the positive reversal type compared to interrupted decrease. This is also what can be observed in general in the whole Ounila watershed. Pixels that had a higher NDVI during the three years before the droughtpoint (see Appendix J, Figure 33) had a higher incidence of the postive reversal type, whereas areas with lower NDVI before the drought breakpoint experienced more interrupted decrease.

4.4.1. Ecosystem response after a flood

The map of flood breakpoints in Figure 14 shows that during the flood period (hydrological year 2015) a breakpoint only occurred in 41.0 % of the pixels. 38.6 % of pixels had a negative breakpoint typology and only 2.3 % of pixels had a positive breakpoint typology. The dominant breakpoint type was the interrupted decrease. In the upper part of the watershed almost no breakpoints occurred, the flooding seems to have had little impact on ecosystem functioning in this region. This becomes apparent in Figure 15 as well, since the land-use types that are more heavily represented in the north of the case study area (sparse vegetation and grassland) have about 70% of pixels without a breakpoint during the flood period. More pixels follow a positive breakpoint typology in the upper part of the watershed than in the lower part, especially the interrupted increase and positive reversal typologies occur in patches. The areas that showed particular greening or browning (Figure 6, Area A-E) contained little breakpoints, in particular the land near Tighza (B) contained almost no breakpoints (Appendix K, Figure 35). In the lower part of the watershed the majority of pixels have experienced an interrupted decrease breakpoint following the drought. This corresponds to the higher occurrence of barren areas in the south, the percentage of pixels without breakpoints for this land use class is lower (48.4%) and the amount of breakpoints with an interrupted decrease is higher (45.9%) than for the other land use classes.

In general, it can be concluded that after both climatic disturbances more negative breakpoints occurred in the lower part of the watershed than in the upper part. During the flooding period as well as during the drought, the interrupted decrease is the dominant breakpoint in the north.

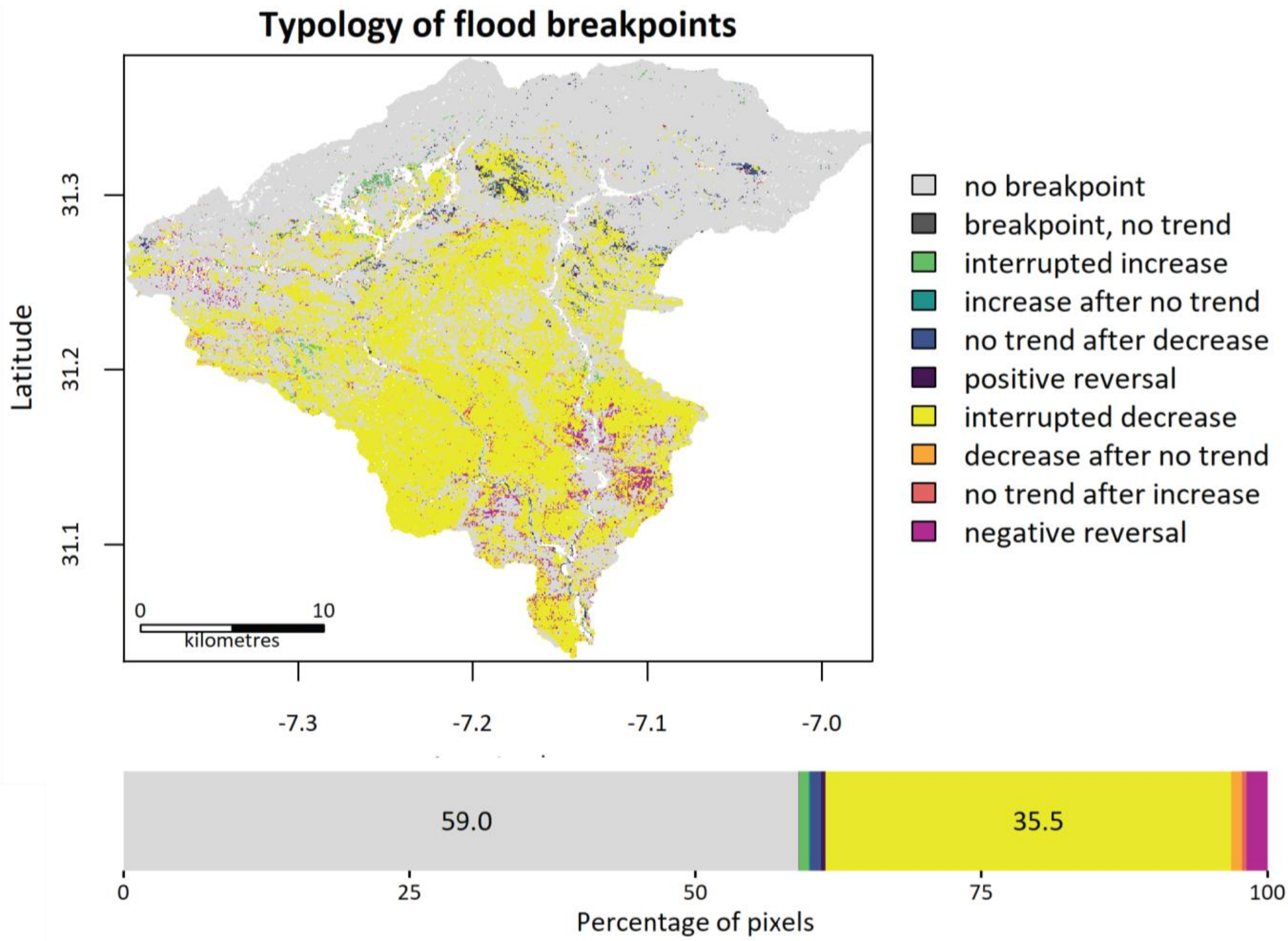

FIGURE 14 | MAP OF THE OUNILA WATERSHED WITH THE TYPOLOGY OF BREAKPOINTS THAT OCCURRED DURING THE FLOOD PERIOD (HYDROLOGICAL YEAR 2015). BELOW THE MAP: BAR WITH THE PERCENTAGE OF PIXELS THAT FOLLOW A CERTAIN TYPOLOGY.

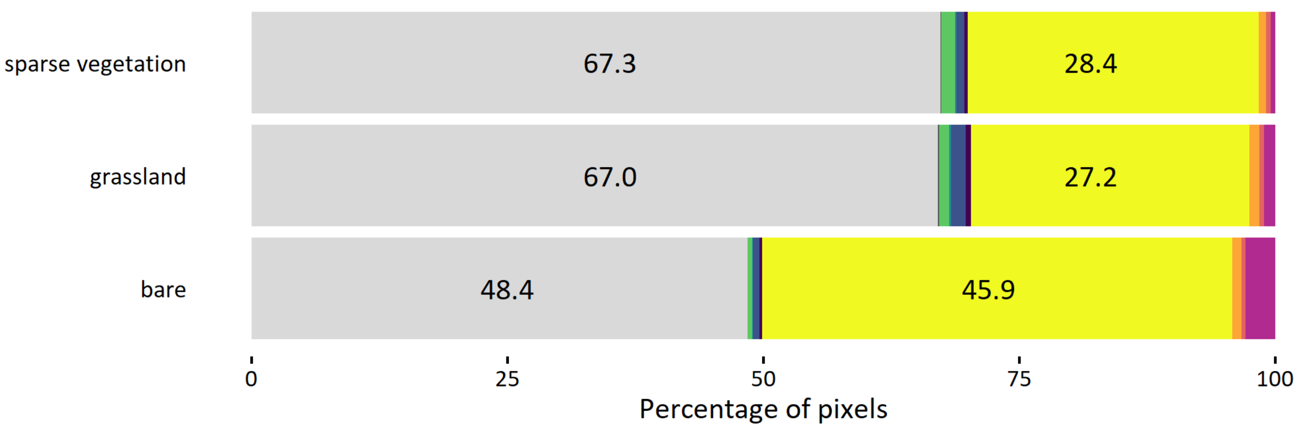

FIGURE 15 | BAR WITH THE PERCENTAGE OF PIXELS THAT FOLLOW A CERTAIN BREAKPOINT TYPOLOGY FOR EACH OF THE MAJOR LAND USE CLASSES: SPARSE VEGETATION, GRASSLAND, CROPLAND AND BARE AREAS.

5. Discussion

5.1. Ecological stability in the Ounila watershed

In general, vegetation cover in the Ounila watershed is low and exhibits very little seasonality, as is often the case in drylands (Watts and Laffan, 2014). In the upper part of the Ounila watershed there has been more change in NDVI, both in negative and positive direction, than in the lower part of the watershed. Some of the patches that experienced greening were cropland or tree plantations, but considerable greening also occurred in areas covered by sparse vegetation or grassland. The observed greening of cropland, along the river channel and in the north-west, is in accordance with the general shift towards irrigated agriculture in the Atlas Mountains observed by El Aich (2018).

In the upper northern part of the watershed the number of negative breakpoints was low, indicating high resistance to abrupt changes towards a deterioration in ecosystem functioning. During the first three years of the monitoring period, NDVI was high in these parts of the watershed too. The higher resistance may be explained by the more vegetated state that the ecosystem was already in. However, it is also important to note that the slopes are very steep in this region. It may be the case that these lands are less accessible to the herds and therefore have experienced a lower grazing intensity. The dominant breakpoint type during the drought in the upper part of the watershed was the positive reversal. In general, the pixels that experienced a positive breakpoint during the drought had a higher vegetation cover during the three years preceding the drought breakpoint. These is in line with observations from von Keyserlingk et al. (2021), who found that higher recovery rates are associated with higher values of NDVI before the drought, in their assessment of a Mediterranean dryland.

Several areas that showed greening were studied in more detail. All these areas were located close to settlements (Area A, C and D are close to Telouet, Area E is located south-east of Anguelz). Resistance to abrupt negative changes in ecosystem functioning was found to be low in these areas, as there was a relatively high number of negative breakpoints present. Given that these areas showed an overall greening throughout the monitoring period, it was expected that they might represent potential hotspots of ecological stability, however the low resistance in these areas does not confirm this. The dominant breakpoint type during the drought was the positive reversal (area A and D) or no breakpoint (C and E). In the area south-east of Anguelz (E) there were also quite a few pixels that experienced an interrupted decrease during the drought. The response of the ecosystem to climatic disturbances indicates high variability: there simultaneously is a high number of abrupt changes towards improvement (positive breakpoints) and deterioration (negative breakpoints) of ecosystem functioning. These areas, that had relatively high initial NDVI and showed overall greening, are neither hotspots of low or high ecological stability. Possibly, ecological stability is impaired by grazing, which may enlarge the width of the range of environmental conditions under which a catastrophic shift can occur (the transitional regime) (Schneider and Sonia, 2016). The fact that these greened areas, that could be referred to as “islands of fertility”, are located in the lower-lying areas presents another indication that these parts of the watershed are in the transitional regime. When the surrounding land is degraded, enhanced run-off causes concentration of resources in patches of more vegetated land (Holmgren and Scheffer, 2001). At the same time, this leads to less resource availability for the surrounding lands, further encouraging the formation of vegetation patches (Kéfi et al., 2007; Rietkerk et al., 2004). In conclusion, there are indications the lands surrounding the settlements of Telouet and Anguelz are currently in a bi-stable state. Therefore, they are at risk of a catastrophic shift towards a barren state. However, it also makes them potential hotspots for land restoration efforts that might move the system to a more stable, vegetated state. These efforts may especially be effective when carried out in parallel with a period of heavy precipitation, for instance during an El Niño episode (Scheffer et al., 2005; Sietz et al., 2017).

In the bare areas located in the centre-east of the watershed, resistance was lowest. In these same areas the interrupted decrease was the dominant breakpoint type during the drought and during the flood period. It can be concluded that ecological stability in the bare areas is low. Initial NDVI during the first three years was low for the bare areas. Not surprisingly, the NDVI before the flood and drought breakpoints was low as well. Most likely, the ecosystem was already in a barren, stable state, before the onset of the monitoring period. This is in accordance with de Keersmaecker et al. (2015), who found that, in a modelling study on a global scale, regions that are sensitive to drought and have a high percentage of bare soil have slow recovery after a disturbance and high "vegetation memory" (their response to disturbances mimics the previous response of the ecosystem).

Interestingly, the degrading lands near Tighza have high resistance to abrupt changes towards deterioration of ecosystem functioning. The dominant breakpoint type is the positive reversal. One patch of land, north of Tighza (located in north-west of Area B), shows other results. Here resistance was high, and vegetation experienced an interrupted decrease during the drought period. This same area had higher NDVI during three years before the drought breakpoint than the surrounding areas, where resistance was high and the response to drought positive. It is curious that the pixels with lower NDVI before the drought show higher ecological stability than the pixels that were more vegetated. It could be that the grazing intensity in the more vegetated areas has been higher, lowering the ecological stability of that area.

It is remarkable that the positive reversal is the most frequently occurring breakpoint category triggered during the drought across all major land use types in the Ounila watershed. This means that in the Ounila watershed, where the ecosystem is water-limited, ecosytem functioning improved after the drought. In general, vegetation cover decreases in dryland ecosystems after a drought (Lotsch et al., 2005). This is in line with what was observed in the bare areas of the centre-east of the case study area, but not with the dominance of positive reversal in the upper half of the watershed. Bernardino et al. (2020) found a similar dominance of the positive reversal breakpoint type in Central Asia (north-west of Caspian Sea). In their case study, this could be related to changes in land management which led to diminished agricultural activities and grazing intensity. Perhaps, a change in land management, for instance in the form of a different grazing regime occurred after the drought. Indeed, the findings of Nieboer (2019) indicate that shepherds have moved their herds further away from the settlements due to land degradation.

In contrast, the dominant breakpoint type after the flood is the interrupted decrease. In a dryland ecosystem where vegetation-growth is water-limited it might be expected that a climatic disturbance with increased precipitation would induce positive breakpoints. The theory that heavy precipitation events might push a degraded ecosystem towards the transitional regime, where recovery towards a vegetated shift may be triggered, can not be confirmed by these results. Apparently, the heavy precipitation alone was not enough to induce such a shift.

5.2. Indicators based on breakpoint typologies to assess ecological stability

The correlation between total number of positive and negative breakpoints did not have a uniform sign and was dependent on location. The hypothesis that positive and negative breakpoints are negatively correlated with each other can not be confirmed based on these results. This means that total number of breakpoints can not straightforwardly be related to one dimension of ecological stability. If positive and negative breakpoints are negatively corelated with each other, a higher ratio of positive to negative breakpoints may indicate that the system resists changes towards a deterioration in ecosystem functioning but not changes that represent an improvement. If this is the case, the total number of breakpoints is hard to interpret as it is an accumulation of two proxies that have different meaning for ecosystem functioning. When the two are positively correlated, this would mean that in areas where there are more abrupt changes towards a deterioration in ecosystem functioning there are more abrupt changes that represent an improvement in ecosystem functioning as well. In that case, the total number of breakpoints would describe the variability of ecosystem functioning, rather than the resistance of the ecosystem towards degradation. In conclusion, the inverse of the total number of breakpoints is not an optimal indicator for ecological stability as it not clear to which dimension of ecological stability it relates. In contrast, the inverse of the total number of negative breakpoints can be used as a proxy of resistance.

The use of a breakpoint typology to describe ecosystem response to climatic disturbances, instead of focusing on the recovery rate adds valuable information. It gives additional insight into the state of the ecosystem before the abrupt change in ecosystem functioning and whether this change has represented an improvement or deterioration. The breakpoint typology could be expanded to include a distinction between accelerating and slowing down trends to be able to differentiate even more between improvements and deteriorations in ecosystem functioning. The effect size of the trends should also be incorporated, to be able to determine the relative importance of such a change in trend. With the method used in this study, hardly any breakpoint of the types containing non-significant trends were detected. Very small trends were significant, because of the high number of observations (between 1200 and 1600 for most pixels, see Appendix B, Figure 20). De Jong et al. (2013) used an arbitrary threshold of 0.25% to distinguish positive and negative trends from no trend. No such threshold was used in this research. Establishing a threshold to distinguish between trends that can be considered stable and trends with meaningful positive or negative magnitude and incorporating this threshold in the classification of breakpoints would be an improvement.

5.3 The use the BFAST method in a dryland ecosystem

It is obvious from the results that the magnitude of NDVI and overall trends in NDVI are very small in the Ounila watershed. The magnitude of change may be small compared to the noise signal in the time-series, making the BFAST method less reliable. BFAST is validated for cases where the noise signal is not bigger than the magnitude of change, however it is not shown to be robust when this is not the case (Verbesselt et al., 2010a). Verbesselt et al. (2010b) postulated that a seasonal amplitude of at least 0.1 is needed to have a sufficient signal-to-noise ratio to generate valid results, assuming that the noise ratio is equal to or greater than 0.1. When the signal to noise ratio is below one there is a higher chance that phenological changes go undetected. There is no risk for false positives (the detection of a breakpoint that is not there). In the data of this study, in 88.8 percent of pixels one or more breakpoints were detected, indicating that the methodology used was rather successful in detecting phenological changes. In addition, Watts and Laffan (2014) applied BFAST to almost aseasonal data, comparable to the data in this study, and validated the BFAST method to detect abrupt changes in dryland ecosystems. It can, therefore, be concluded that the BFAST method has been effective in detecting abrupt changes in the case study area. However, in the pixels with extremely low NDVI and seasonal amplitude, some breakpoints may have gone undetected. It is also worth noting that the Landsat 8 data has better signal to noise ratio than the data from Landsat 4-7, which may have led to a slightly higher chance for detection of breakpoints in the part of the time-series were Landsat 8 data is included (2013 – present).

Although an effort was made to base the value of the h parameter on scientific literature and some manual inspections of the data it was not feasible to carry out a sensitivity analysis on the full case study area due to computational limitations. Future case studies that utilize the BFAST method would benefit form a generic study on appropriate h-values across biomes for different data densities.

In this study, no assessments were based on the exact determination of the breakpoint date because it was deemed not robust. The accuracy of the determination of the timing of phenological changes, such as breakpoints, is dependent on the temporal resolution and the incidence of missing data (Zhang et al., 2009).The data that was used in this research was very irregular. This means that the chance of detecting a breakpoint is expected to be impacted by the data density at the given time. When there is more data available, there is a higher chance of detecting a breakpoint in that period. Therefore, the exact timing of breakpoints is not robust for irregular time-series. For the method chosen in this research, this has not impacted the results because it focused on the total number of breakpoints. Since the amount of observations in the case study area is roughly equal throughout the case study area it is not expected to have impacted the spatial analysis on total number of breakpoints or the distribution of drought and flood breakpoints. Only in the north-eastern limit of the watershed data availability was much lower. It is important to note that the number of breakpoints, positive or negative, and the occurrence of drought and flood breakpoints was lower there too. Possibly, breakpoints have gone undetected due to the by lower data density in that area.

5.5. Future research directions

Verbesselt et al. (2010a) recommend that Landsat images can best be used in combination with satellite images from other sources, such as MODIS, to improve its data coverage and temporal resolution. Future research efforts could focus on creating a multi-sensor time-series of NDVI in which gaps of missing data are imputed. Since the exact timing of breakpoints may then be determined more reliably, this would allow other indicators of ecological stability to be derived from the NDVI data. For instance: the time period between the onset of the drought and the occurrence of a breakpoint. It could be argued that in a healthy ecosystem it would take a longer time for a breakpoint to occur after the drought as healthy vegetation has a buffering capacity. Another interesting indicator would be the amount of days it takes after a drought breakpoint to reach the same NDVI level as before the breakpoint. This is a proxy for critical slowing down. Critical slowing down is the phenomena that occurs when recovery rates decrease as the ecosystem approaches a critical threshold (Scheffer et al., 2015). This can also be quantified using spatial autocorrelation. Verbesselt et al. (2016) found that with precipitation levels that are associated with critical thresholds, spatial autocorrelation increases. It would be interesting to quantify critical slowing down using spatial autocorrelation in periods of low precipitation in the watershed. Incorporating more indicators of ecological stability will improve the understanding of this multi-dimensional concept. When doing so in future research, it also important to study the correlations between the multiple dimensions of ecological stability (Donohue et al., 2016).

Investigating ecological stability on other organisational levels, will lead to a more complete understanding of ecosystem functioning (Kéfi et al., 2019). In addition, direct advice on land management can not be obtained from results purely based on satellite data. For these reasons, the findings of this research should be complemented with field observations. Species diversity and soil properties such as soil texture and type are known to control the response of ecosystem functioning to droughts and other disturbances (Maestre et al., 2016). These data can be used to validate the findings of this research and provide further insight in the ecosystem functioning. Soil moisture content can be measured in the field to identify those areas that have the highest potential for successful land management interventions. Seneviratne et al. (2010) argue that the direction of feedbacks between vegetation and atmosphere are dependent on the soil moisture regime. When the soil moisture content is in the transitional regime, a small intervention can move the system towards a healthier vegetated state. In addition, it would be good to have a more exact picture of the distribution of precipitation levels in the watershed so that local differences in rainfall can be taken into account. Using rainfall gauges to measure precipitation would be beneficial. Finally, the land use map that was used in this research is a prototype map for the whole African continent, that has not yet been validated in the field. To obtain a better understanding of the land cover types present in the Ounila watershed, information on land cover and vegetation types should be obtained from the field.

This study has resulted in the identification of hotspots of high and low ecological stability and has given indications of areas with high potential for land restoration. This provides valuable insight in order to prevent land degradation and may aid in the development of land management strategies based on ecological stability. However, to gain a better understanding of the drivers behind ecological stability, it is very important that the grazing intensity in the watershed is quantified. Future research should focus on mapping the grazing intensity and its development over time in the Ounila watershed. The most effective method for mapping current grazing intensity would be to use GPS-tracking on the herds that are present in the watershed. To reconstruct a map of past grazing intensity a participatory mapping approach could be applied (Altmann et al., 2018; Ramirez Gómez, 2019; Wario et al., 2015). Alternatively, grazing intensity can be determined as the inverse distance from grazing hotspots, such as drinking points or settlements (Manthey and Peper, 2010). In addition to vegetation cover and grazing regime, geomorphological features such as slope and aspect are important determinants of ecosystem functioning and may control the effects of climatic disturbances on ecosystems (Maestre et al., 2016). Therefore, it would be interesting to explore the relationships between these potential drivers and the indicators of ecological stability more in depth.

5. Conclusions

In this study, ecological stability was successfully quantified using newly developed indicators based on the typology of abrupt changes in response to climatic disturbances. This has provided insight on the hotspots of low and high ecological stability in the Ounila watershed and potential areas for land restoration. The main findings are:

1. In the upper watershed both greening and browning occurred between 1984 and 2019. Areas that already had very low vegetation in the beginning of the monitoring period, exhibited little change in overall NDVI.
2. Two major climatic disturbances have occurred in the Ounila watershed: a drought (hydrological years 1999 – 2002) and a flood period (hydrological year 2015).
3. The ecosystem was more resistant to abrupt changes, leading to a deterioration in ecosystem functioning, in the upper, more vegetated, part of the watershed than in the lower, more barren, part. In the areas that showed greening, resistance was generally low. In contrast, the degraded lands near Tighza had relatively high resistance.
4. In general, the ecosystem has experienced a shift from degrading trends to positive vegetation trends following the drought Especially in the upper part of the watershed this was the dominant breakpoint type. In the bare areas in the lower half of the watershed the trend in NDVI was negative both before and after the drought period as well as the flood period, indicating continued land degradation.

Ecological stability in the Ounila watershed is higher in the grasslands of the upper north and low in the bare areas in the centre-east and south of the watershed. In regions that showed relatively high or low ecological stability (i.e. high resistance and improvement in ecosystem functioning in response to climatic disturbance and low resistance and deterioration in ecosystem functioning in response to climatic disturbance, respectively), this could be related to initial NDVI and land cover type. Areas with low initial NDVI and a high fraction of bare land typically showed low ecosystem stability, whereas areas with high initial NDVI and higher fraction of more vegetated land use types (grassland or sparse vegetation) showed relatively high ecological stability. Most interesting are the areas, close to the settlements, that experienced particular greening or browning throughout the monitoring period. The areas that experienced greening had low resistance but a general improvement in ecosystem functioning in response to drought. **The greened areas are not hotspots of ecological stability, but may indicate high potential for land restoration in the surrounding areas.** The area near Tighza, that experienced browning, had high resistance and a general improvement in ecosystem functioning in response to drought. With the exception for a small patch north-west of this area, that had low resistance and a negative response to drought.

The findings of this MSc thesis are a first step towards the implementation of stability-based restoration measures in the Ounila watershed. To bridge the gap between the findings from this thesis and implementation, field data and information on grazing intensity should be obtained to complement these results.

Acknowledgements

I am thankful to my supervisor, Àngeles Garcia Mayor, who inspired me with her extensive knowledge on dryland ecosystems and for her guidance in this research. I would like to thank my second supervisor, Saskia Förster, who provided me with great feedback and helpful advice regarding the methodology of this research. I also want to express my appreciation to Robert Behling who consulted me on the processing of Landsat satellite images. I want to thank Jennifer von Keyserlingk for her work in developing the "resInd" package and her willingness to help me develop it even further. I am grateful to Myrna de Hoop for the insightful conversations regarding data analysis. Finally, I would like to thank Latifa Oumlil for providing me with information on the case study area and doing such great work with PermaAtlas.

References

Altmann, B.A., Jordan, G., Schlecht, E., 2018. Participatory mapping as an approach to identify grazing pressure in the Altay Mountains, Mongolia. Sustain. 10, 1–15. https://doi.org/10.3390/su10061960

Beck, H.E., Zimmermann, N.E., McVicar, T.R., Vergopolan, N., Berg, A., Wood, E.F., 2018. Present and future Köppen-Geiger climate classification maps at 1-km resolution. Sci. Data 5, 1–12. https://doi.org/10.1038/sdata.2018.214

Benassi, M., 2008. Drought and climate change in Morocco . Analysis of precipitation field and water supply. Drought Manag. Sci. techinological Innov. A, 83–86.

Bernardino, P.N., De Keersmaecker, W., Fensholt, R., Verbesselt, J., Somers, B., Horion, S., 2020. Global-scale characterization of turning points in arid and semi-arid ecosystem functioning. Glob. Ecol. Biogeogr. 29, 1230–1245. https://doi.org/10.1111/geb.13099

Buckley, S.M., Agram, P.S., Belz, J.E., Crippen, R.E., Gurrola, E.M., Kobrick, M., Lavalle, M., Martin, J.M., Neumann, M., Nguyen, Q.D., Rosen, P.A., Shimada, J.G., Simard, M., Tung, W.W., 2020. NASADEM.

Copernicus, 2020. Agrometeorological indicators from 1979 to 2018 derived from reanalysis [WWW Document]. Clim. Data Store. https://doi.org/10.24381/cds.6c68c9bb

de Jong, R. De, Verbesselt, J., Zeileis, A., Schaepman, M.E., 2013. Shifts in Global Vegetation Activity Trends 1117–1133. https://doi.org/10.3390/rs5031117

De Keersmaecker, W., Lhermitte, S., Tits, L., Honnay, O., Somers, B., Coppin, P., 2015. A model quantifying global vegetation resistance and resilience to short-term climate anomalies and their relationship with vegetation cover. Glob. Ecol. Biogeogr. 24, 539–548. https://doi.org/10.1111/geb.12279

Donohue, I., Hillebrand, H., Montoya, J.M., Petchey, O.L., Pimm, S.L., Fowler, M.S., Healy, K., Jackson, A.L., Lurgi, M., McClean, D., O'Connor, N.E., O'Gorman, E.J., Yang, Q., 2016. Navigating the complexity of ecological stability. Ecol. Lett. 19, 1172–1185. https://doi.org/10.1111/ele.12648

El Aich, A., 2018. Changes in livestock farming systems in the Moroccan Atlas Mountains. Open Agric. 3, 131–137. https://doi.org/10.1515/opag-2018-0013

European Space Agency, 2017. Land Cover CCI Product User Guide Version 1.1.

Evans, J.S., 2020. spatialEco.

Grimm, V., Wissel, C., 1997. Babel, or the ecological stability discussions: An inventory and analysis of terminology and a guide for avoiding confusion. Oecologia 109, 323–334. https://doi.org/10.1007/s004420050090

Hodgson, D., Mcdonald, J.L., Hosken, D.J., 2015. What do you mean , "resilient"? Trends Ecol. Evol. 30, 503–506. https://doi.org/10.1016/j.tree.2015.06.010

Holling, C.S., 1996. Engineering Resilience versus Ecological Resilience, in: Schulze, P.C. (Ed.), Engineering Within Ecological Constraints. National Academy of Engineering, pp. 31–44.

Holling, C.S., 1973. Resilience and Stability of Ecological Systems. Annu. Rev. Ecol. Syst. 4, 1–23.

Holmgren, M., Scheffer, M., 2001. El Niño as a window of opportunity for the restoration of degraded arid ecosystems. Ecosystems 4, 151–159. https://doi.org/10.1007/s100210000065

IPCC, 2018. Summary for Policymakers, Global warming of 1.5°C. An IPCC Special Report on the impacts of global warming of 1.5°C above pre-industrial levels and related global greenhouse gas emission pathways, in the context of strengthening the global response to the threat of climate change,. Geneva, Szwitzerland. https://doi.org/10.1017/CBO9781107415324

Jax, K., 2005. Function and ‘“ functioning ”’ in ecology : what does it mean ? 3, 641–648.

Kéfi, S., Domínguez-García, V., Donohue, I., Fontaine, C., Thébault, E., Dakos, V., 2019. Advancing our understanding of ecological stability. Ecol. Lett. 22, 1349–1356. https://doi.org/10.1111/ele.13340

Kéfi, S., Rietkerk, M., Alados, C.L., Pueyo, Y., Papanastasis, V.P., ElAich, A., De Ruiter, P.C., 2007. Spatial vegetation patterns and imminent desertification in Mediterranean arid ecosystems. Nature 449, 213–217. https://doi.org/10.1038/nature06111

Lotsch, A., Friedl, M.A., Anderson, B.T., Tucker, C.J., 2005. Response of terrestrial ecosystems to recent Northern Hemispheric drought. Geophys. Res. Lett. 32, 1–5. https://doi.org/10.1029/2004GL022043

LP DAAC, n.d. Data Pool [WWW Document]. USGS Earth Resour. Obs. Sci. Cent. URL https://lpdaa.usgs.gov/tools/data-pool/ (accessed 4.10.20).

Maestre, F.T., Eldridge, D.J., Soliveres, S., Kéfi, S., Delgado-Baquerizo, M., Bowker, M.A., García-Palacios, P., Gaitán, J., Gallardo, A., Lázaro, R., Berdugo, M., 2016. Structure and Functioning of Dryland Ecosystems in a Changing World. Annu. Rev. Ecol. Evol. Syst. 47, 215–237. https://doi.org/10.1146/annurev-ecolsys-121415-032311

Maestre, F.T., Salguero-Gómez, R., Quero, J.L., 2012. It is getting hotter in here: Determining and projecting the impacts of global environmental change on drylands. Philos. Trans. R. Soc. B Biol. Sci. 367, 3062–3075. https://doi.org/10.1098/rstb.2011.0323

Manthey, M., Peper, J., 2010. Estimation of grazing intensity along grazing gradients - the bias of nonlinearity. J. Arid Environ. 74, 1351–1354. https://doi.org/10.1016/j.jaridenv.2010.05.007

McKee, T.B., Doesken, N.J., Kleist, J., 1993. The relationship of drought frequency and duration to time scales, in: Eighth Conference on Applied Climatology. Department of Atmopsheric Science, Colorado State University, Anaheim, California, pp. 178–184.

Millennium Ecosystem Assessment, 2005. Ecosystems and Human Well-being: Desertification Synthesis. Washington, DC.

Nes, E.H. Van, Scheffer, M., 2007. Slow Recovery from Perturbations as a Generic Indicator of a Nearby Catastrophic Shift. Am. Nat. 169, 738–747.

Nieboer, S., 2019. Possibilities for a sustainable grazing system in Anguelz , Morocco , and the implementation with public participation. Utrecht University.

Ponce Campos, G.E., Moran, M.S., Huete, A., Zhang, Y., Bresloff, C., Huxman, T.E., Eamus, D., Bosch, D.D., Buda, A.R., Gunter, S.A., Scalley, T.H., Kitchen, S.G., Mcclaran, M.P., Mcnab, W.H., Montoya, D.S., Morgan, J.A., Peters, D.P.C., Sadler, E.J., 2013. Ecosystem resilience despite large-scaled altered hydroclimatic conditions. Nature 494, 349–352. https://doi.org/10.1038/nature11836

Povoa, L. V., Nery, J.T., 2016. precintcon: Precipitation Intensity, Concentration and Anomaly Analysis.

Prăvălie, R., 2016. Drylands extent and environmental issues. A global approach. Earth-Science Rev. 161, 259–278. https://doi.org/10.1016/j.earscirev.2016.08.003

Radiant Design Sarl, n.d. Dossier technique d’un système anti érosion pour le vallon Abalh, Douar Anguelz Ounila, Commune de Télouet, Province de Ouarzazate.

Ramirez Gómez, S.O.I., 2019. Land voices in land use decisions: Co-producing spatial knowledge on ecosystem services with indigenous and tribal communities in intact forest regions. Universiteit Utrecht.

Reynolds, J.F., Stafford Smith, D.M., Lambin, E.F., Turner, B.L., Mortimore, M., Batterbury, S.P.J., Downing, T.E., Dowlatabadi, H., Fernández, R.J., Herrick, J.E., Huber-Sannwald, E., Jiang, H., Leemans, R., Lynam, T., Maestre, F.T., Ayarza, M., Walker, B., 2007. Ecology: Global desertification: Building a science for dryland development. Science (80-.). 316, 847–851. https://doi.org/10.1126/science.1131634

Rietkerk, M., Dekker, S.C., De Ruiter, P.C., Van De Koppel, J., 2004. Self-organized patchiness and catastrophic shifts in ecosystems. Science (80-.). 305, 1926–1929. https://doi.org/10.1126/science.1101867

Roy, D.P., Kovalskyy, V., Zhang, H.K., Vermote, E.F., Yan, L., Kumar, S.S., Egorov, A., 2016. Remote Sensing of Environment Characterization of Landsat-7 to Landsat-8 re fl ective wavelength and normalized difference vegetation index continuity. Remote Sens. Environ. 185, 57–70. https://doi.org/10.1016/j.rse.2015.12.024

RStudio Team, 2018. RStudio: Integrated Development for R.

Scheffer, M., Carpenter, S., Foley, J.A., Folke, C., Walker, B., 2001. Catastrophic shifts in ecosystems 413.

Scheffer, M., Carpenter, S.R., 2003. Catastrophic regime shifts in ecosystems: Linking theory to observation. Trends Ecol. Evol. 18, 648–656. https://doi.org/10.1016/j.tree.2003.09.002

Scheffer, M., Carpenter, S.R., Dakos, V., Nes, E.H. Van, 2015. Generic Indicators of Ecological Resilience : Inferring the Chance of a Critical Transition. Annu. Rev. Ecol. Evol. Syst. 46, 145–167. https://doi.org/10.1146/annurev-ecolsys-112414-054242

Scheffer, M., Holmgren, M., Brovkin, V., Claussen, M., 2005. Synergy between small- And large-scale feedbacks of vegetation on the water cycle. Glob. Chang. Biol. 11, 1003–1012. https://doi.org/10.1111/j.1365-2486.2005.00962.x

Schneider, F.D., Sonia, K., 2016. Spatially heterogeneous pressure raises risk of catastrophic shifts. Theor. Ecol. 9, 207–217. https://doi.org/10.1007/s12080-015-0289-1

Seneviratne, S.I., Corti, T., Davin, E.L., Hirschi, M., Jaeger, E.B., Lehner, I., Orlowsky, B., Teuling, A.J., 2010. Investigating soil moisture-climate interactions in a changing climate: A review. Earth-Science Rev. 99, 125–161. https://doi.org/10.1016/j.earscirev.2010.02.004

Sietz, D., Fleskens, L., Stringer, L.C., 2017. Learning from Non-Linear Ecosystem Dynamics Is Vital for Achieving Land Degradation Neutrality. L. Degrad. Dev. 28, 2308–2314. https://doi.org/10.1002/ldr.2732

U.S. Geological Survey, n.d. Dictionary of Water terms [WWW Document]. URL https://www.usgs.gov/special-topic/water-science-school/science/dictionary-water-terms?qt-science_center_objects=0#qt-science_center_objects (accessed 12.22.20).

UNCCD, 2017. Global Land Outlook. First Edition.

USGS/EROS, 2020. LSDS-1417. Earth Resources Observation and Science (EROS) Center Science Processing Architecture (ESPA) On-Demand Interface User Guide Release 3.0.0.

USGS/EROS, 2019. LSDS-1370. Landsat 4-7 Surface Reflectance (LEDAPS) Product Guide. https://doi.org/10.1016/0042-207X(74)93024-3

van Rooy, M.P., 1965. A Rainfall Anomaly Index independent of Time and Space. Notos.

Verbesselt, J., Hyndman, R., Newnham, G., Culvenor, D., 2010a. Detecting trend and seasonal changes in satellite image time series. Remote Sens. Environ. 114, 106–115. https://doi.org/10.1016/j.rse.2009.08.014

Verbesselt, J., Hyndman, R., Zeileis, A., Culvenor, D., 2010b. Phenological change detection while accounting for abrupt and gradual trends in satellite image time series. Remote Sens. Environ. 114, 2970–2980. https://doi.org/10.1016/j.rse.2010.08.003

Verbesselt, J., Umlauf, N., Hirota, M., Holmgren, M., Van Nes, E.H., Herold, M., Zeileis, A., Scheffer, M., 2016. Remotely sensed resilience of tropical forests. Nat. Clim. Chang. 6, 1028–1031. https://doi.org/10.1038/nclimate3108

von Keyserlingk, J., de Hoop, M., Mayor, A.G., Dekker, S.C., Rietkerk, M., Foerster, S., 2021. Resilience of vegetation to drought : studying the effect of grazing in a Mediterranean rangeland using satellite time series 1–50.

Wario, H.T., Roba, H.G., Kaufmann, B., 2015. Shaping the Herders' "Mental Maps": Participatory Mapping with Pastoralists' to Understand Their Grazing Area Differentiation and Characterization. Environ. Manage. 56, 721–737. https://doi.org/10.1007/s00267-015-0532-y

Watts, L.M., Laffan, S.W., 2014. Effectiveness of the BFAST algorithm for detecting vegetation response patterns in a semi-arid region. Remote Sens. Environ. 154, 234–245. https://doi.org/10.1016/j.rse.2014.08.023

Watts, L.M., Laffan, S.W., 2013. Sensitivity of the BFAST algorithm to MODIS satellite and vegetation index. Proc. - 20th Int. Congr. Model. Simulation, MODSIM 2013 1638–1644. https://doi.org/10.36334/modsim.2013.h2.watts

Zeileis, A., Kleiber, C., Krämer, W., Hornik, K., 2002. Testing and dating of structural changes in practice.

Zhang, X., Friedl, M.A., Schaaf, C.B., 2009. Sensitivity of vegetation phenology detection to the temporal resolution of satellite data. Int. J. Remote Sens. 30, 2061–2074. https://doi.org/10.1080/01431160802549237

Appendix A: Ancillary data: elevation, slope and aspect

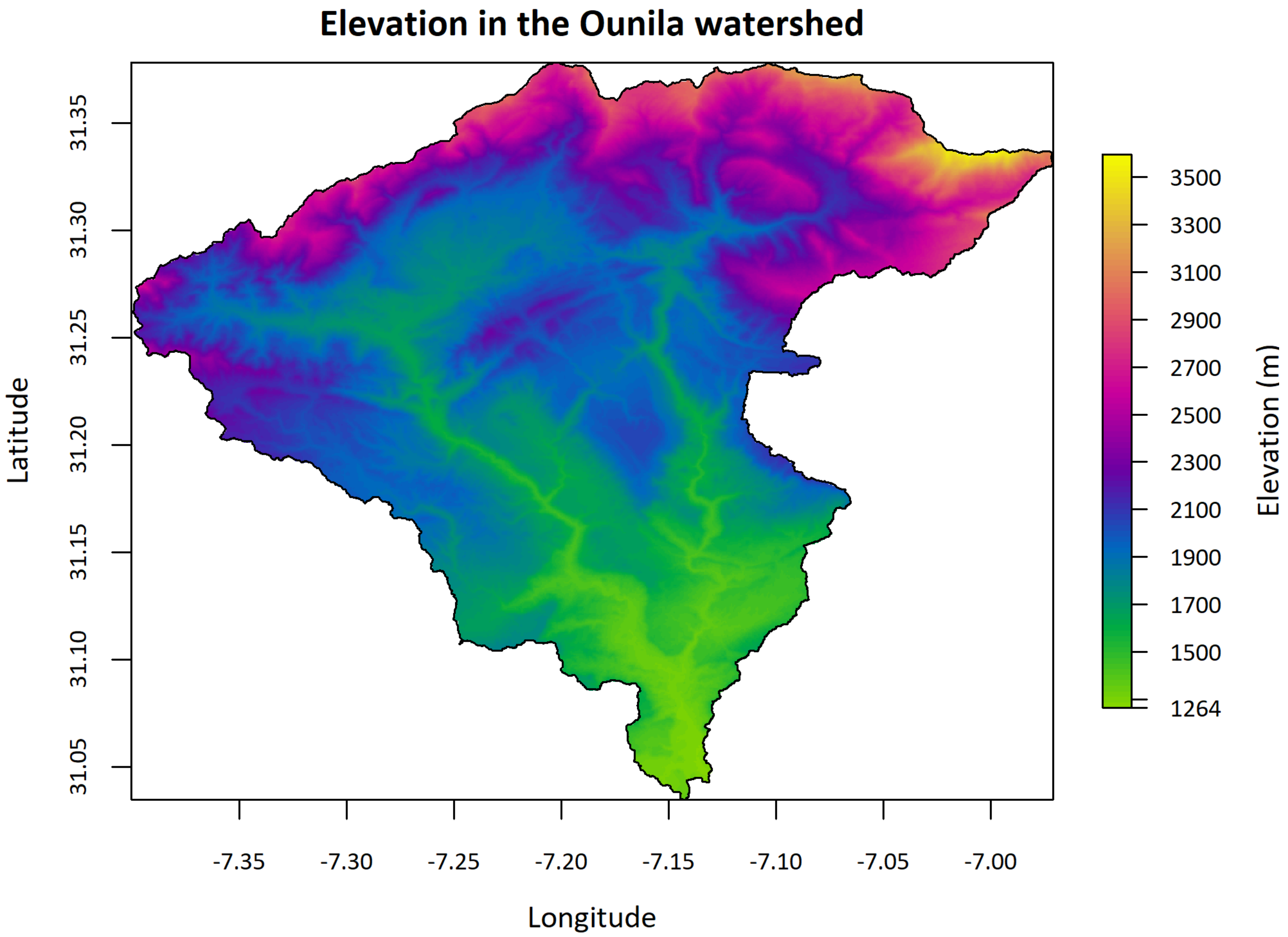

FIGURE 16 | DIGITAL ELEVATION MODEL (DEM) IN THE OUNILA WATERSHED WITH A SPATIAL RESOLUTION OF 30 BY 30 M. DATA FROM THE NASA MAKING EARTH SYSTEM DATA RECORDS FOR USE IN RESEARCH ENVIRONMENTS (MEASUREs) DIGITAL ELEVATION MODEL (DEM) DATASET (BUCKLEY ET AL., 2020).

.

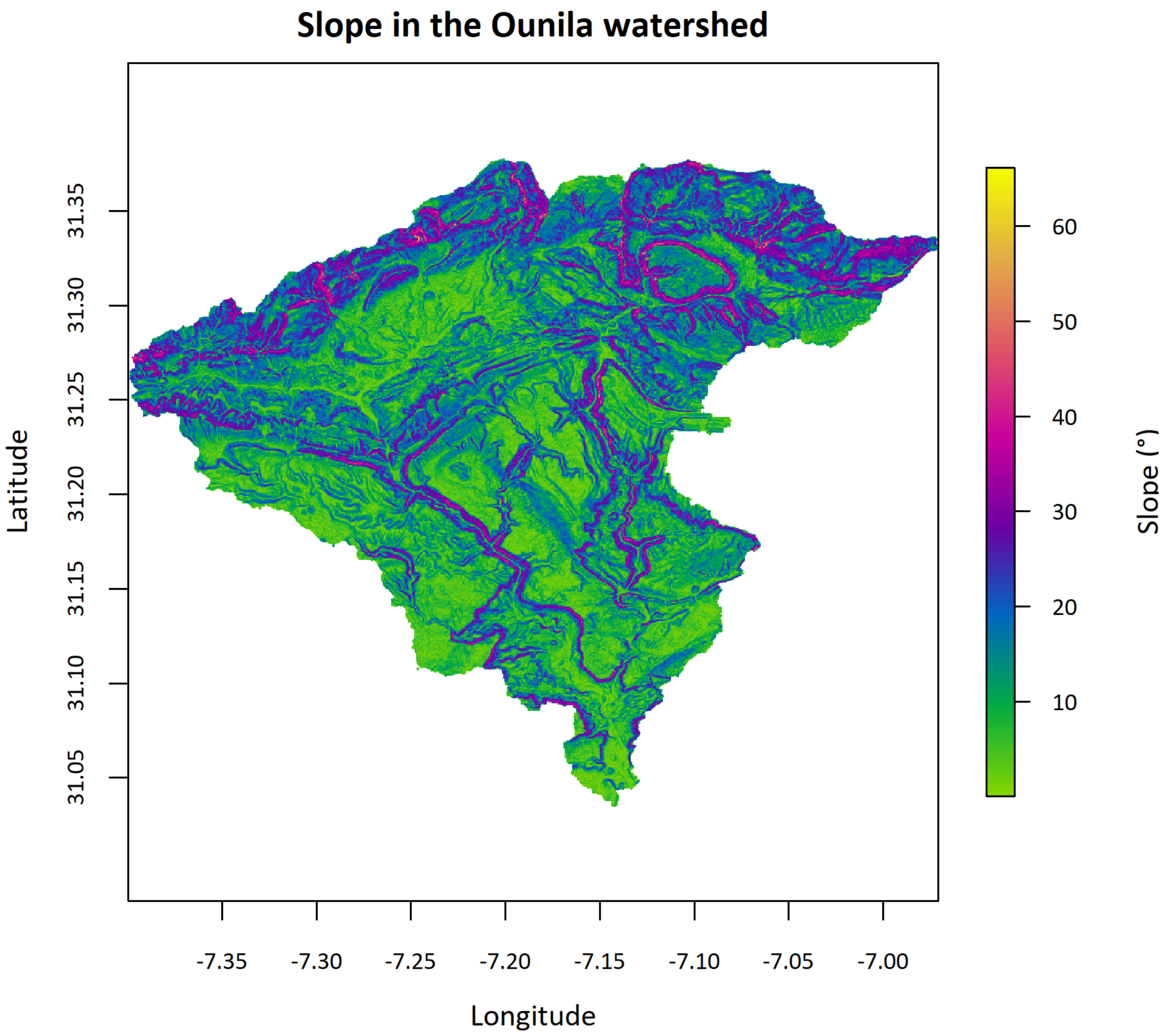

Figure 17 | Slope in the Ounila watershed with a spatial resolution of 30 by 30 m. Data from The NASA Making Earth System Data Records for Use in Research Environments (MEaSUREs) Digital Elevation Model (DEM) dataset (Buckley et al., 2020).

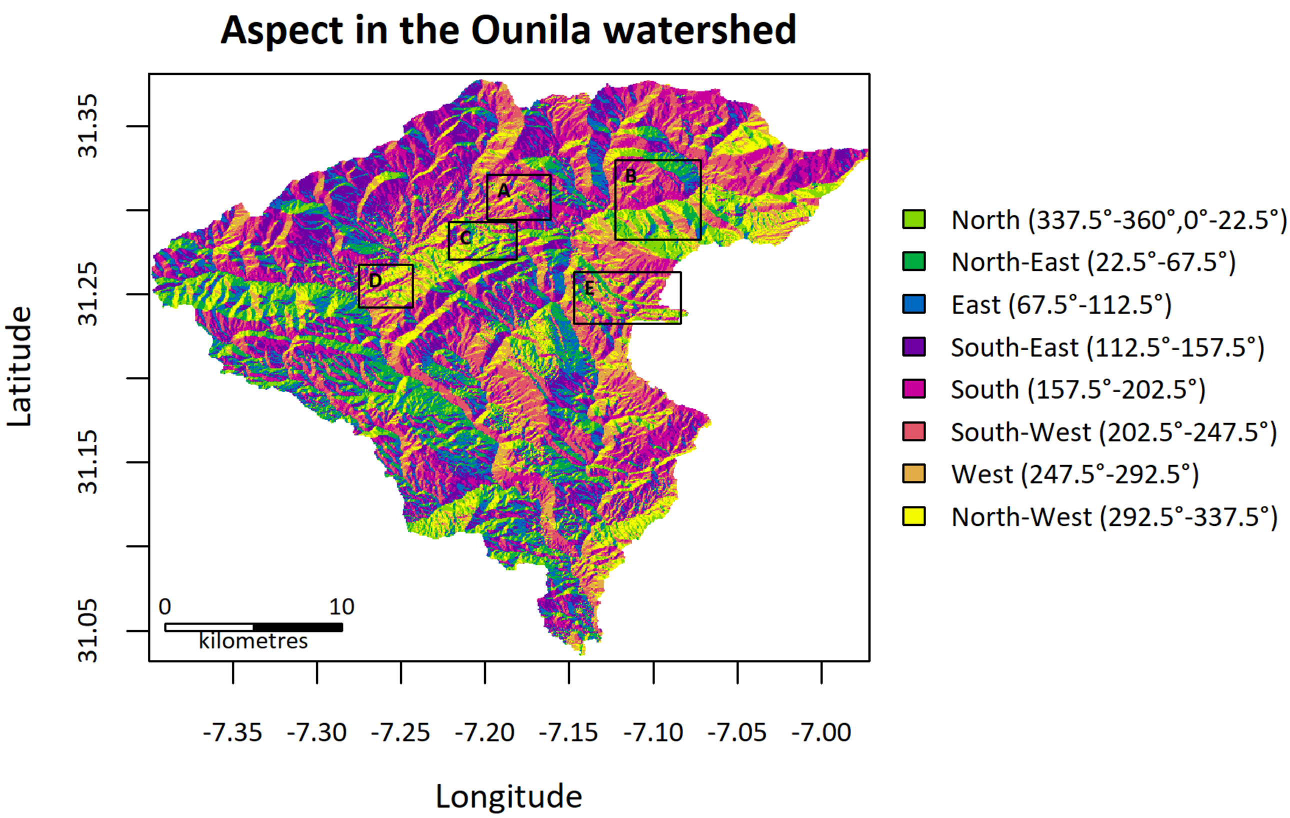

FIGURE 18 | ASPECT (ORIENTATION OF SLOPES) IN THE OUNILA WATERSHED WITH A SPATIAL RESOLUTION OF 30 BY 30 M. DATA FROM THE NASA MAKING EARTH SYSTEM DATA RECORDS FOR USE IN RESEARCH ENVIRONMENTS (MEASURES) DIGITAL ELEVATION MODEL (DEM) DATASET (BUCKLEY ET AL., 2020).

Appendix B: Data density

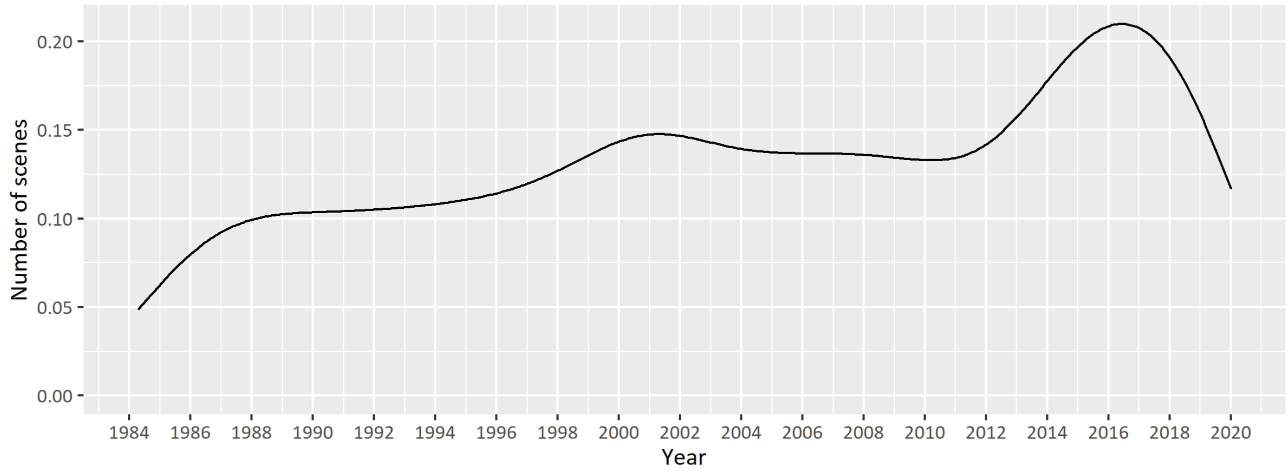

FIGURE 19 | RELATIVE FREQUENCY OF NUMBER OF LANDSAT SCENES OVER TIME

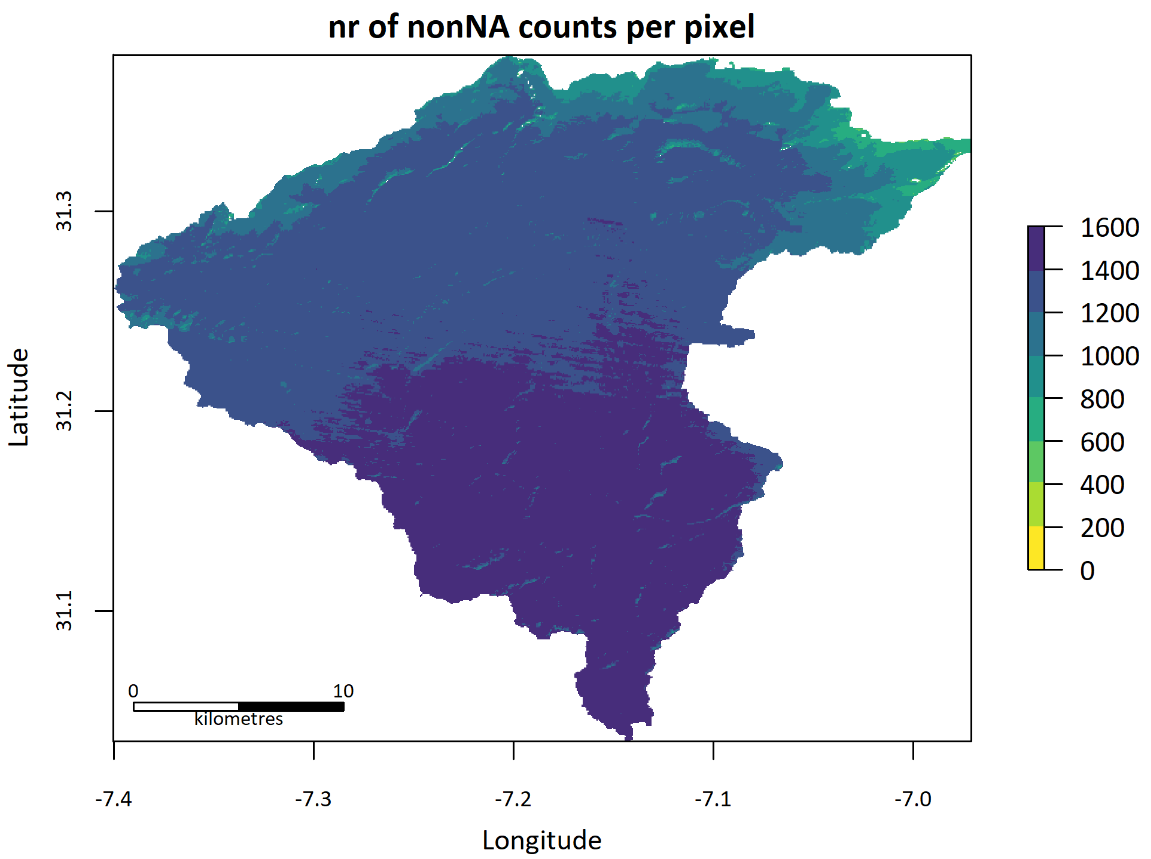

FIGURE 20 | NUMBER OF LANDSAT NDVI OBSERVATIONS THROUGHOUT THE MONITORING PERIOD (2981-2019) PER PIXEL IN THE OUNILA WATERSHED. SPATIAL RESOLUTION IS 30 BY 30 M.

Appendix C: Untransformed NDVI data

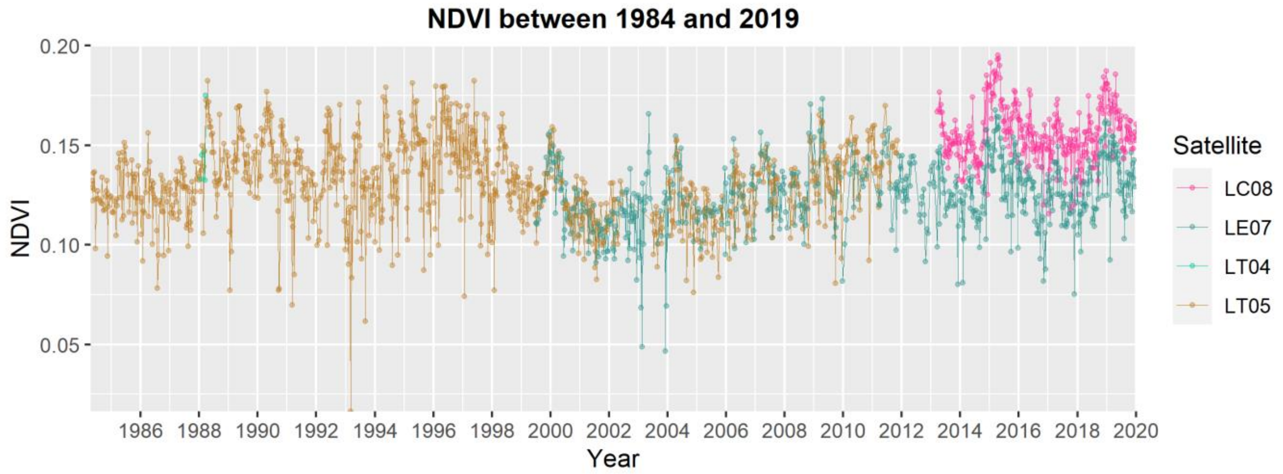

FIGURE 21 | TIME-SERIES OF MEAN NDVI IN THE OUNILA WATERSHED BETWEEN 1984 AND 2019 BEFORE ANY TRANSFORMATION WAS APPLIED TO MAKE THE DATA CONTINUOUS. THE SATELLITE THAT COLLECTED THE DATA IS INDICATED.

Appendix D: Absolute change in NDVI and initial NDVI

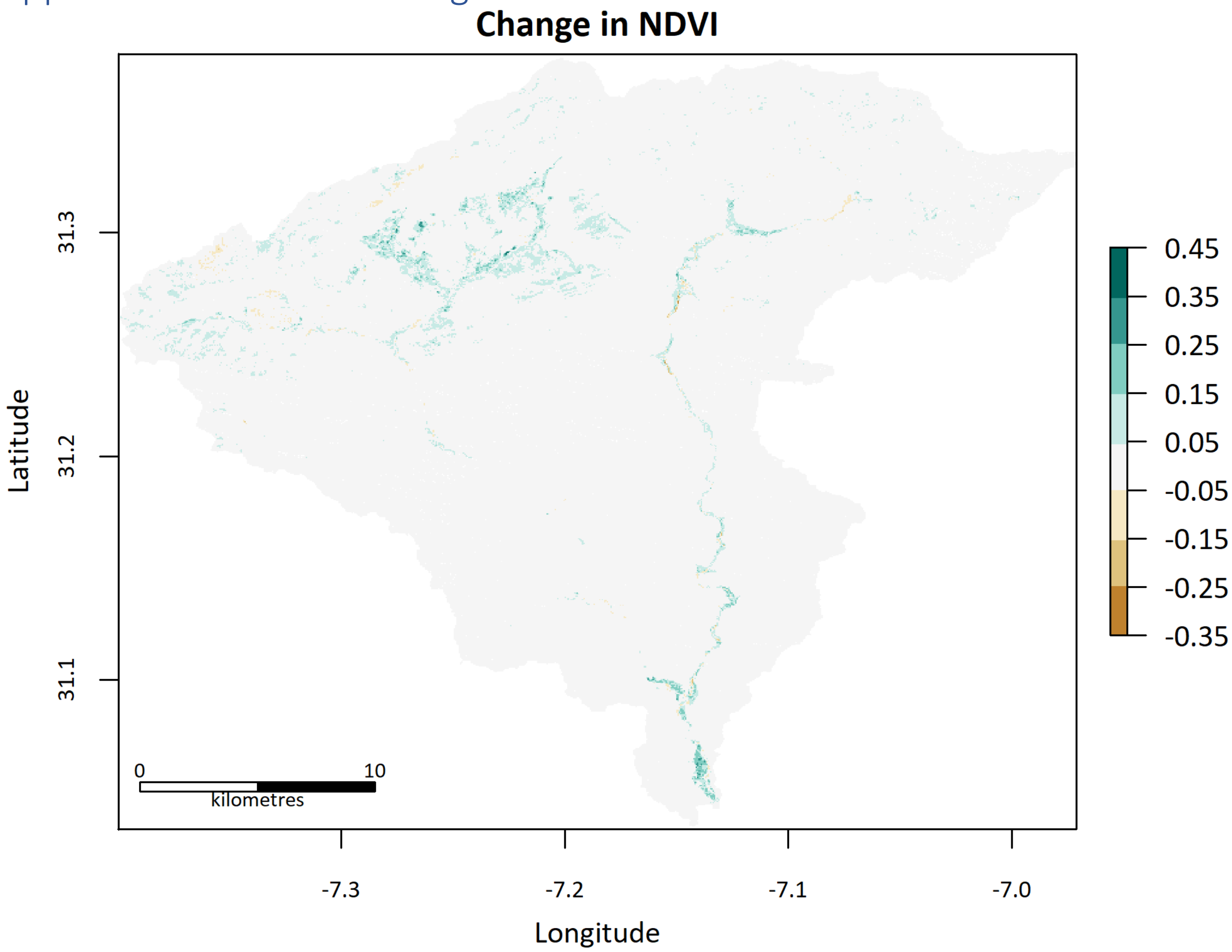

FIGURE 22 | ABSOLUTE CHANGE IN MEAN NDVI DURING THE FIRST THREE YEARS OF THE MONITORING PERIOD (1984-2019) AND THE LAST THREE YEARS, IN THE OUNILA WATERSHED. SPATIAL RESOLUTION IS 30 BY 30 M.

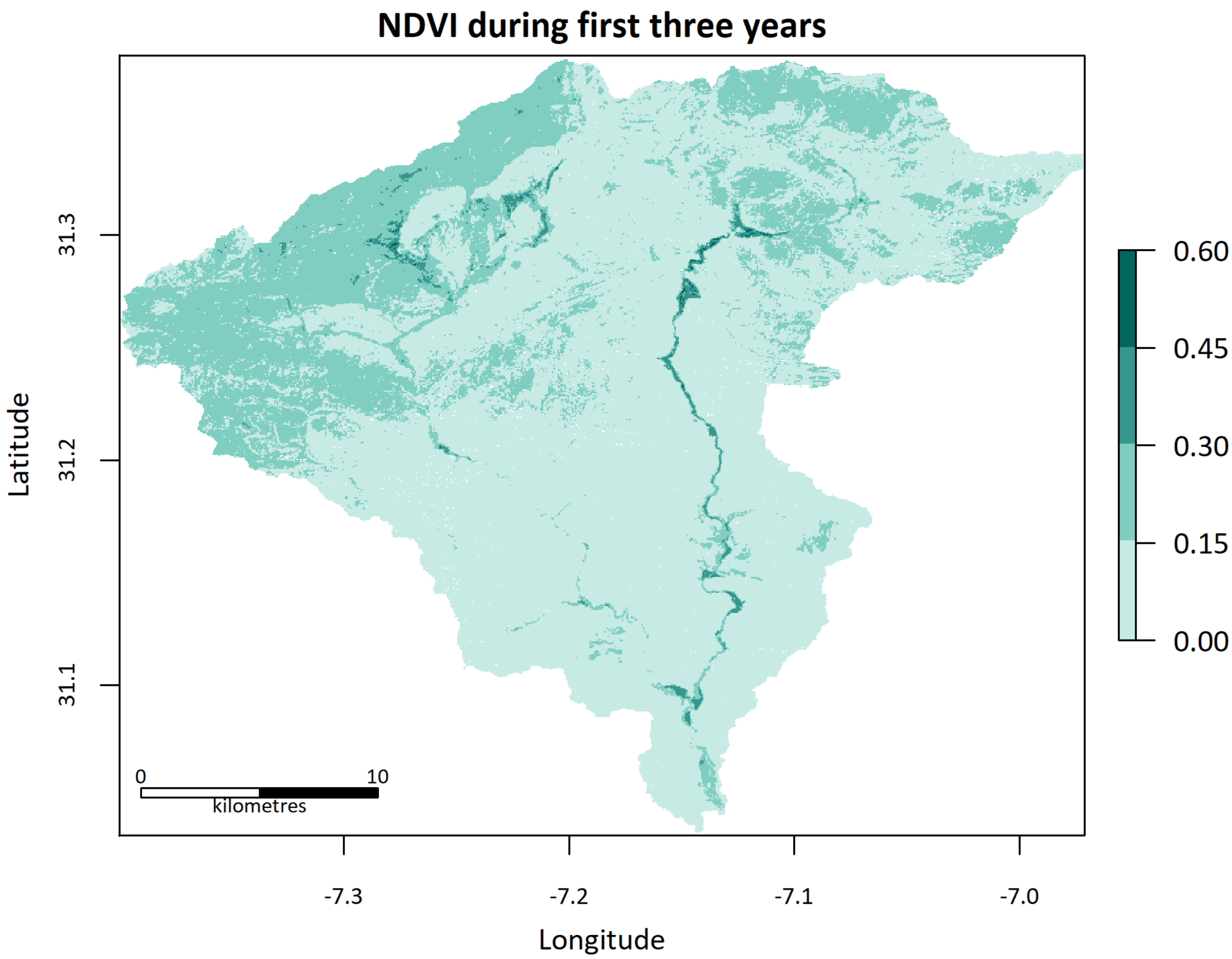

Figure 23 | Initial mean NVDI during the first three years of the monitoring period (1984-2019) in the Ounila watershed. spatial resolution is 30 by 30 m.

Appendix E: Selection of areas of interest

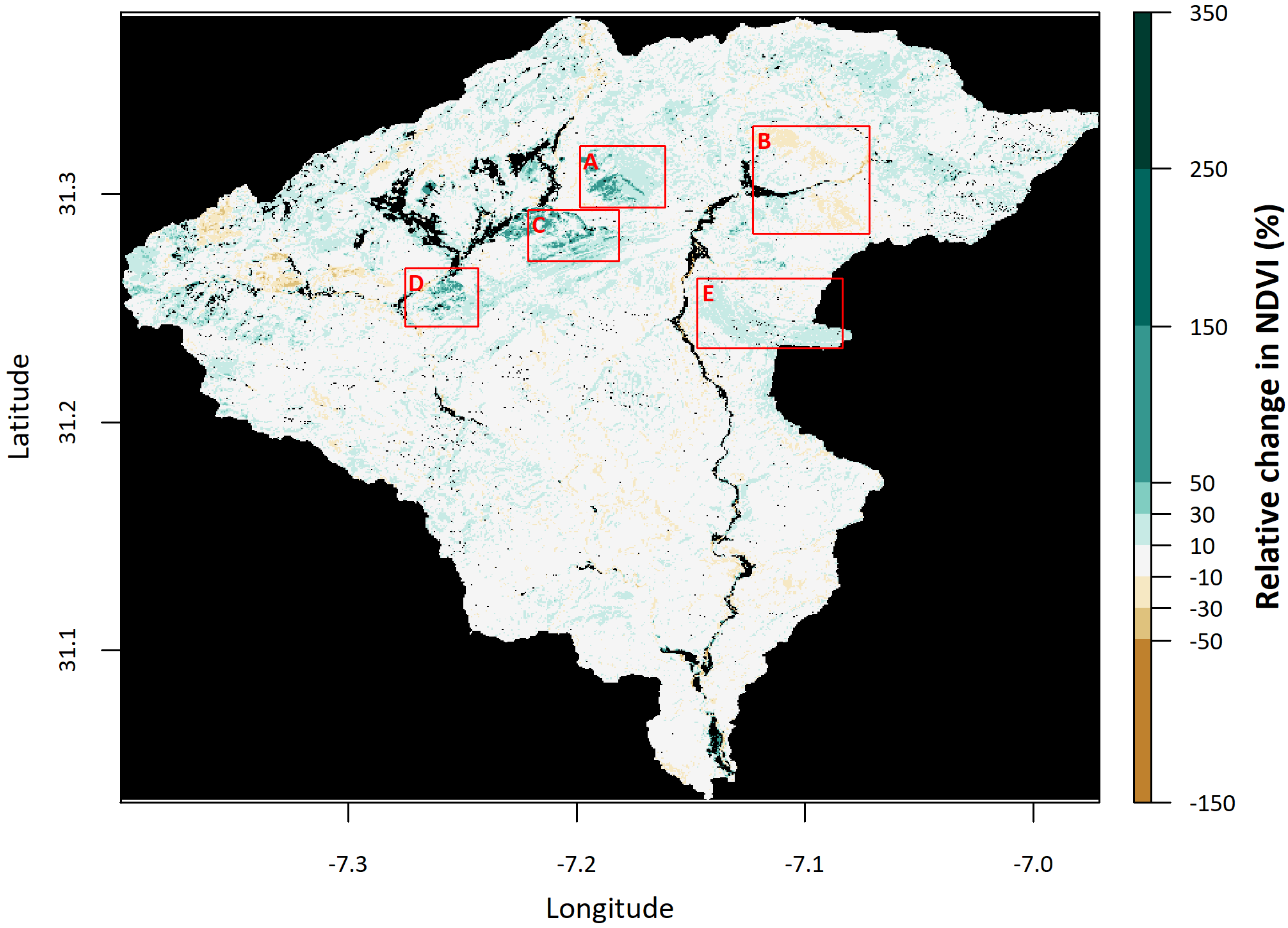

Figure 24 | Relative change in NDVI in the Ounila watershed between the first three years of the monitoring period (1984-2019) and the last three years of the monitoring period. In the red boxes areas of interest are indicated. The croplands are masked out, and pixels with NA-values are black. Spatial resolution is 30 by 30 m.

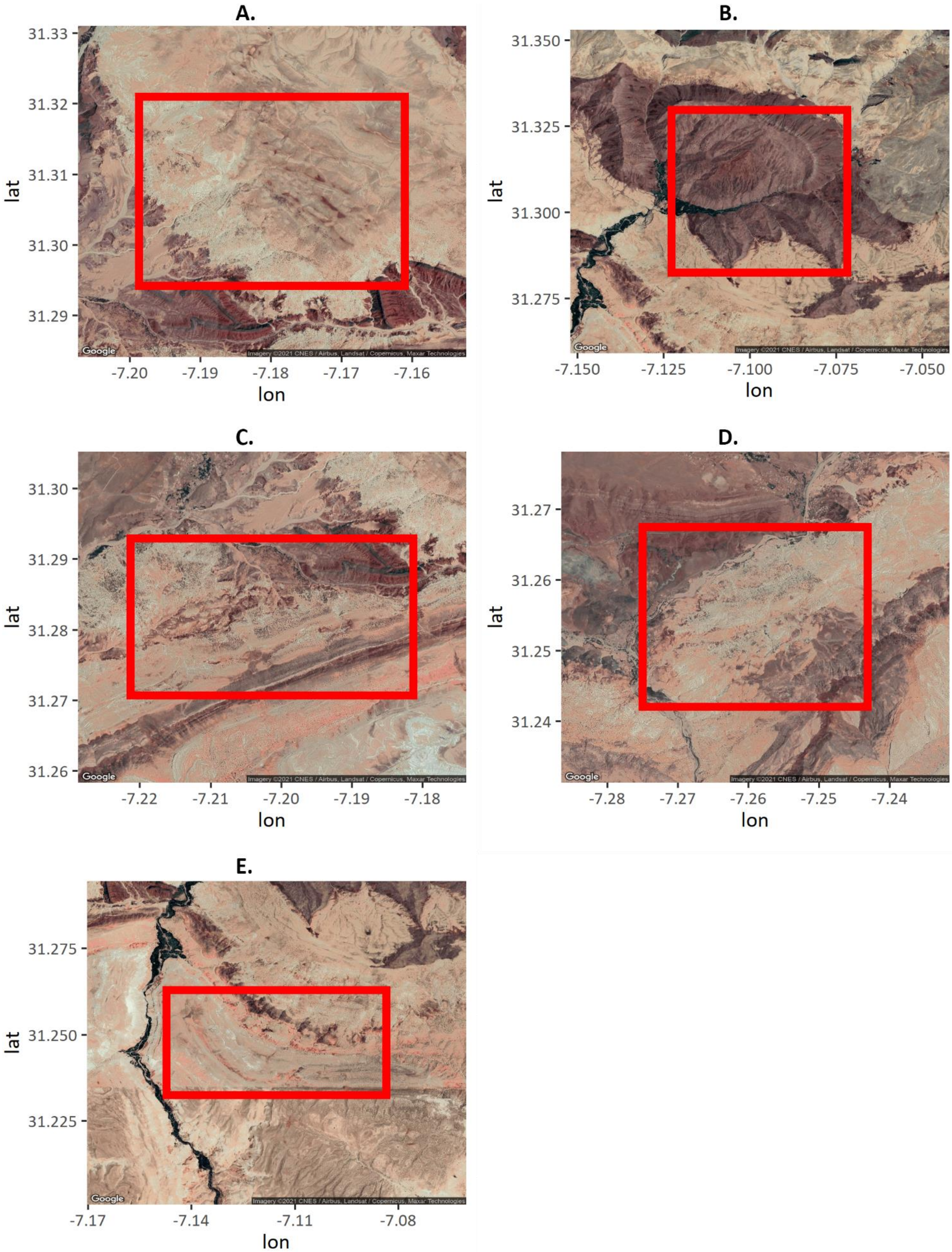

FIGURE 25 | GOOGLE SATTELITE IMAGES OF THE AREAS OF INTEREST: A-E

Appendix F: RAI per hydrological year

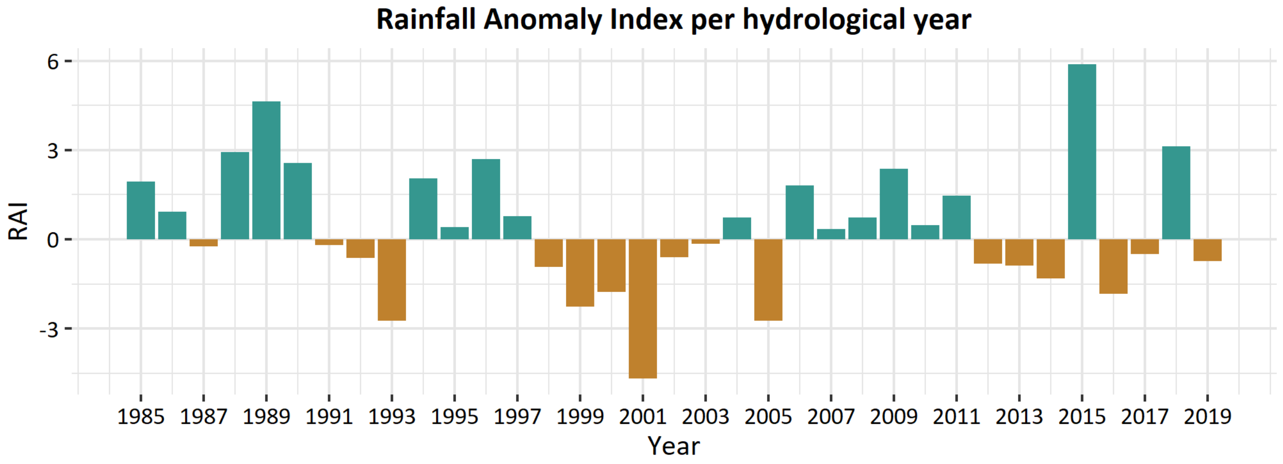

FIGURE 26 | RAINFALL ANOMALY INDEX (FOLLOWING THE METHOD OF VAN ROOY (1965)) PER HYDROLOGICAL YEAR.

Appendix G: Total number of positive and negative breakpoints per type

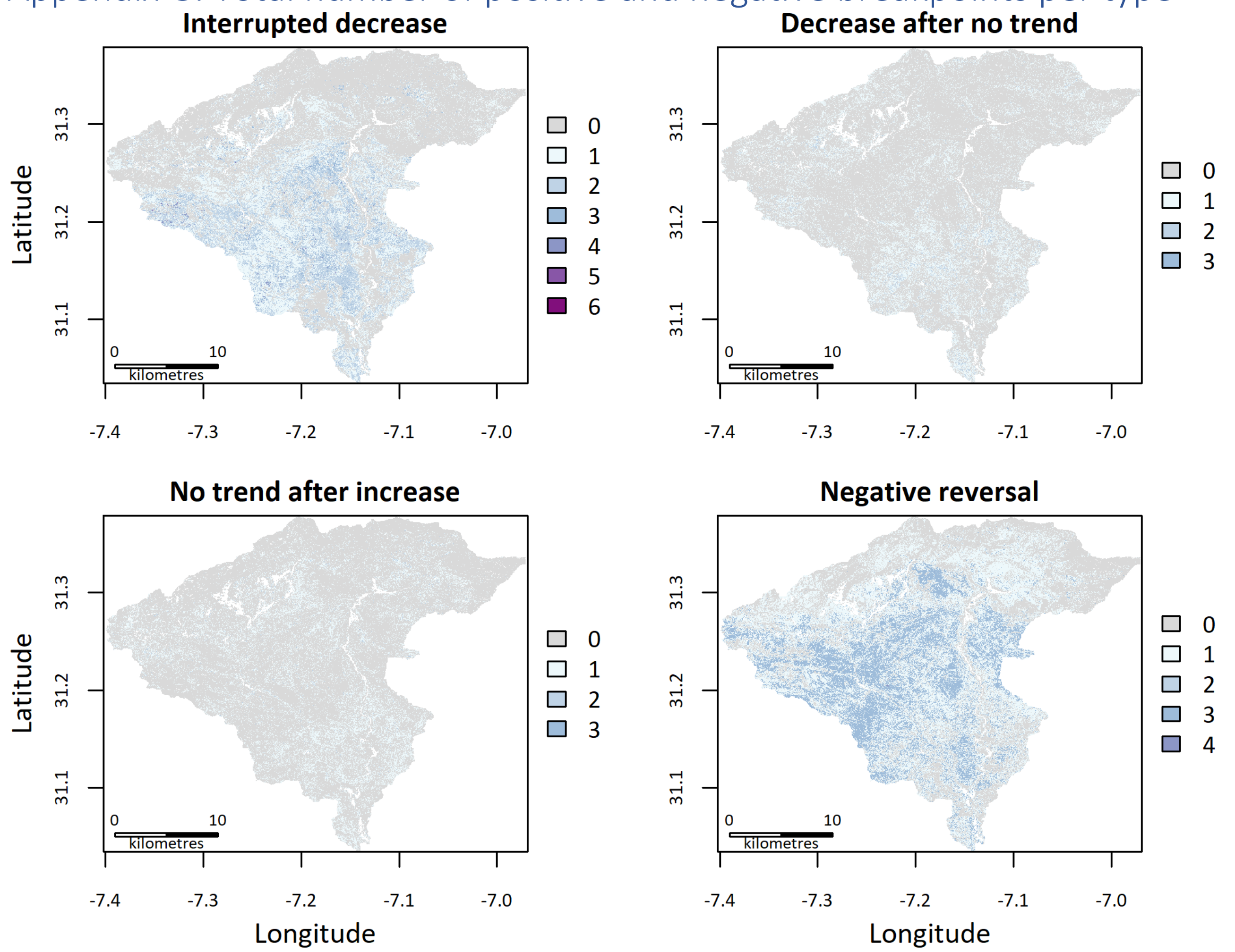

FIGURE 27 | TOTAL NUMBER OF BREAKPOINTS DETECTED BETWEEN 1984 AND 2019 PER NEGATIVE BREAKPOINT TYPE: INTERRUPTED DECREASE, DECREASE AFTER NO TREND, NO TREND AFTER INCREASE AND NEGATIVE REVERSAL. CROPLANDS ARE MASKED OUT. SPATIAL RESOLUTION IS 30 BY 30 M.

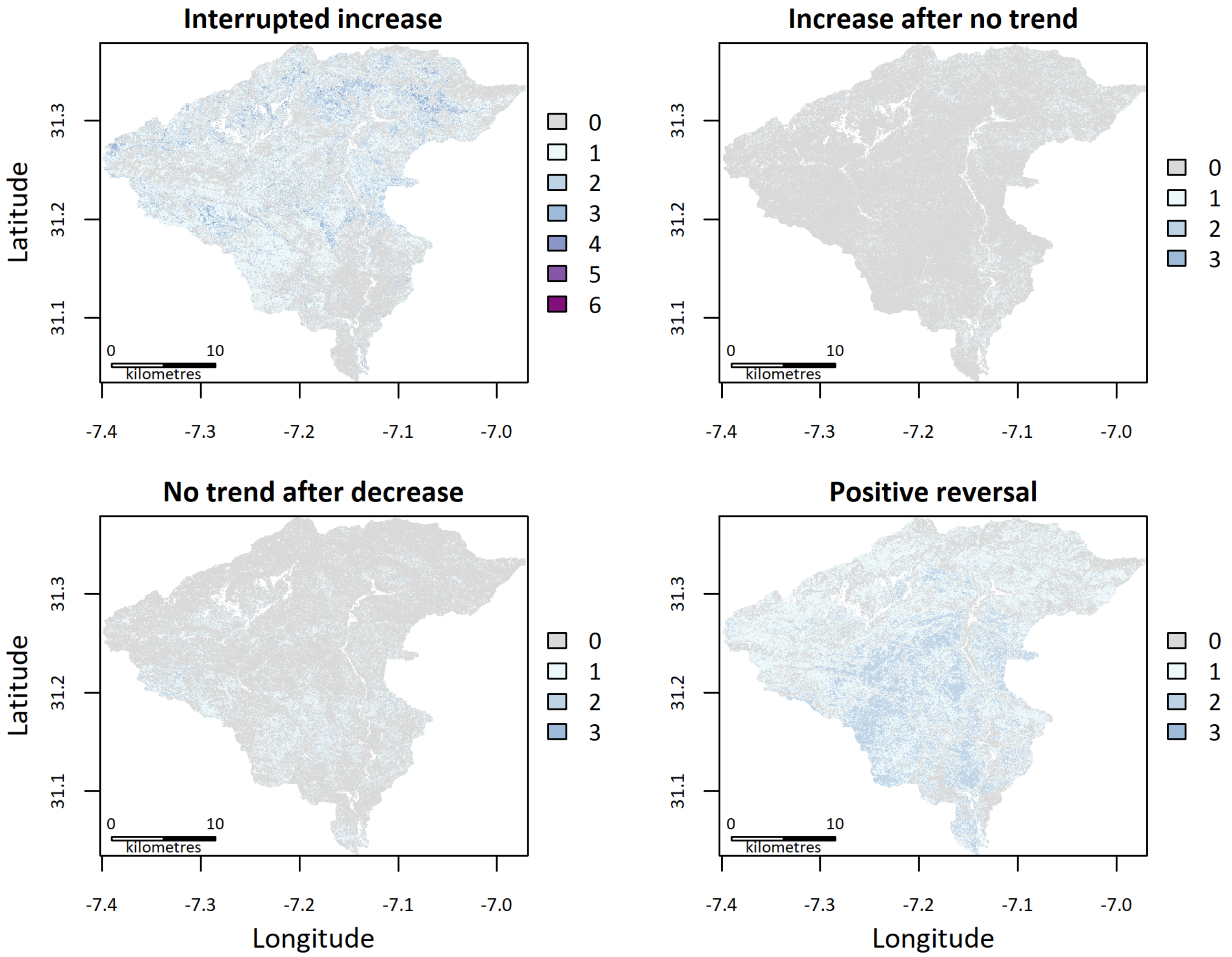

FIGURE 28 | TOTAL NUMBER OF BREAKPOINTS DETECTED BETWEEN 1984 AND 2019 PER POSITIVE BREAKPOINT TYPE: INTERRUPTED INCREASE, INCREASE AFTER NO TREND, NO TREND AFTER DECREASE AND POSITIVE REVERSAL. CROPLANDS ARE MASKED OUT. SPATIAL RESOLUTION IS 30 BY 30 M.

Appendix H: Number of breakpoints per Land Use type

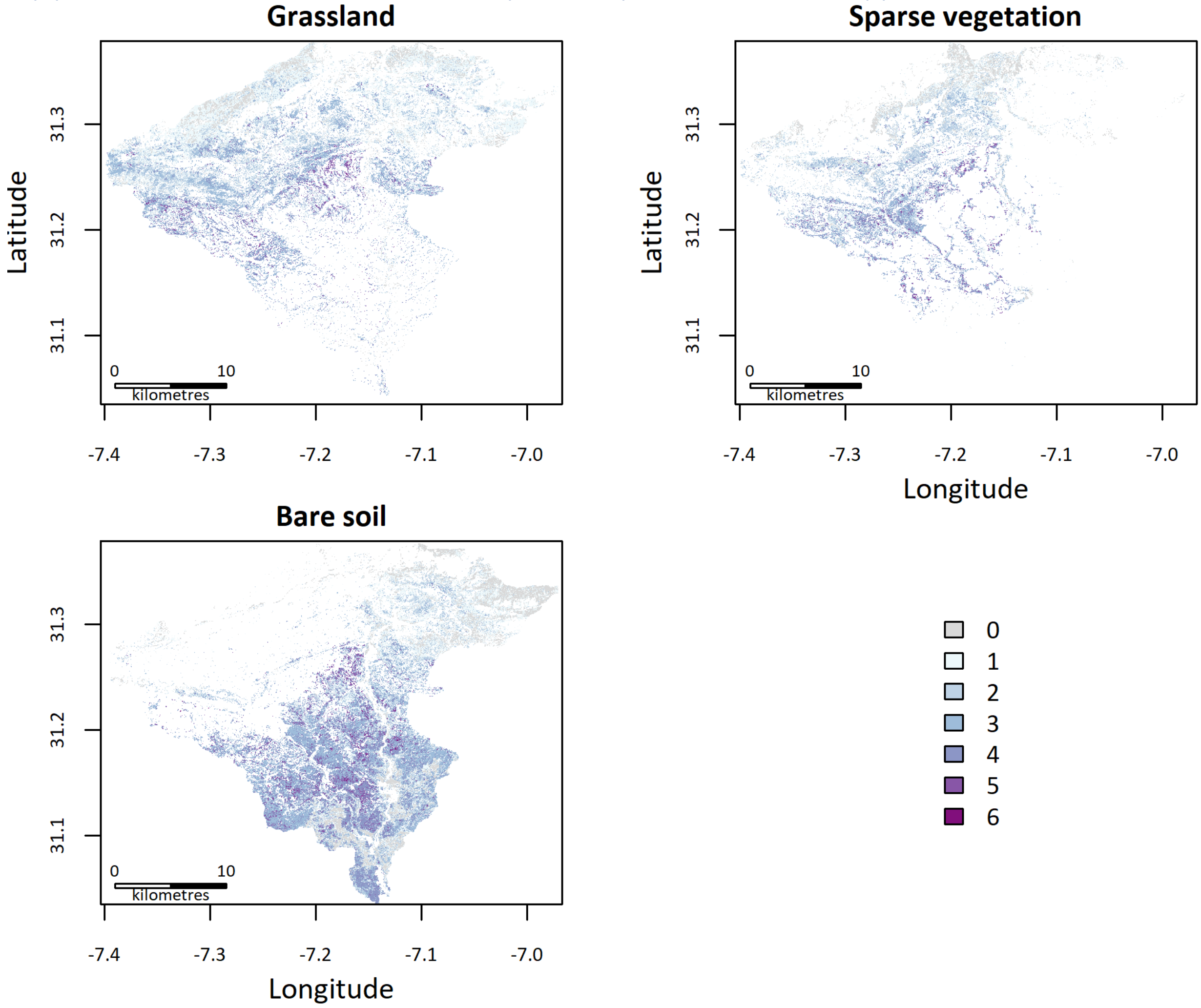

FIGURE 29 | TOTAL NUMBER OF NEGATIVE BREAKPOINTS DETECTED BETWEEN 1984 AND 2019 PER MAJOR LAND USE TYPE IN THE OUNILA WATERSHED: GRASSLAND, CROPLAND, SPARSE VEGETATION AND LICHEN MOSSES AND BARE SOIL. SPATIAL RESOLUTION IS 30 BY 30 M.

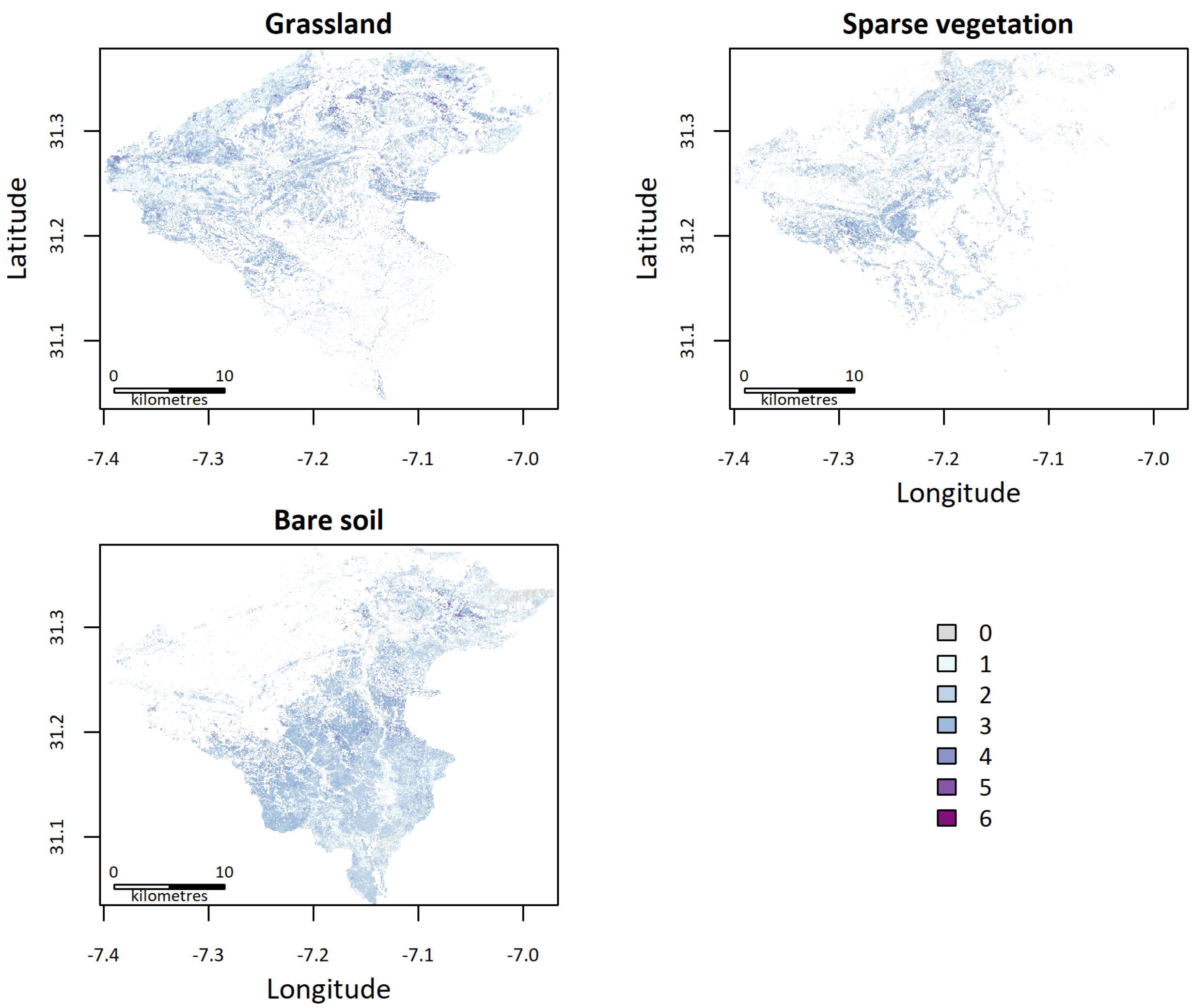

FIGURE 30 | TOTAL NUMBER OF POSITIVE BREAKPOINTS DETECTED BETWEEN 1984 AND 2019 PER MAJOR LAND USE TYPE IN THE OUNILA WATERSHED: GRASSLAND, CROPLAND, SPARSE VEGETATION AND LICHEN MOSSES AND BARE SOIL. SPATIAL RESOLUTION IS 30 BY 30 M.

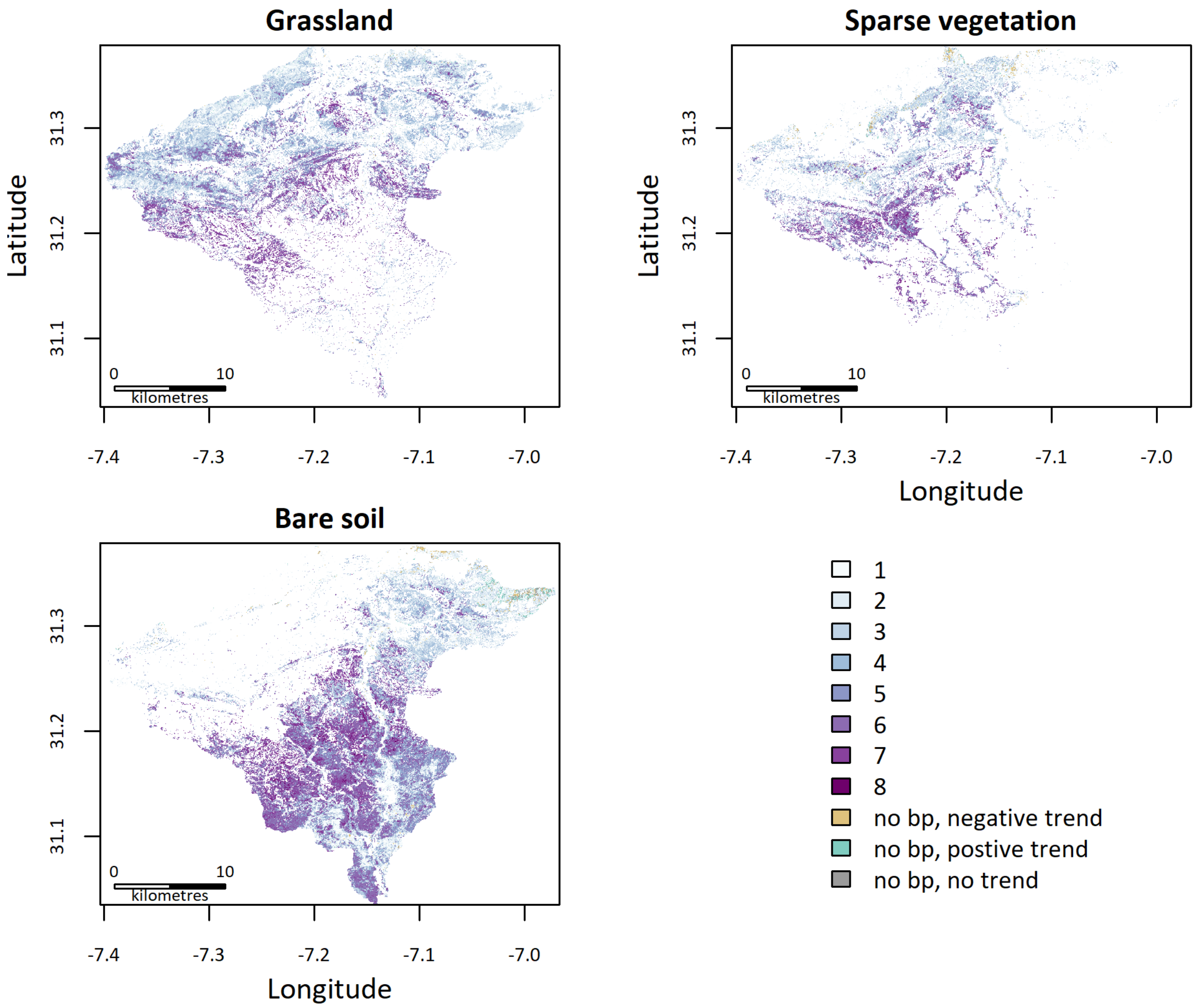

FIGURE 31 | TOTAL NUMBER OF BREAKPOINTS DETECTED BETWEEN 1984 AND 2019 PER MAJOR LAND USE TYPE IN THE OUNILA WATERSHED: GRASSLAND, CROPLAND, SPARSE VEGETATION AND LICHEN MOSSES AND BARE SOIL. SPATIAL RESOLUTION IS 30 BY 30 M.

Appendix I: Total number of positive and negative breakpoints per type

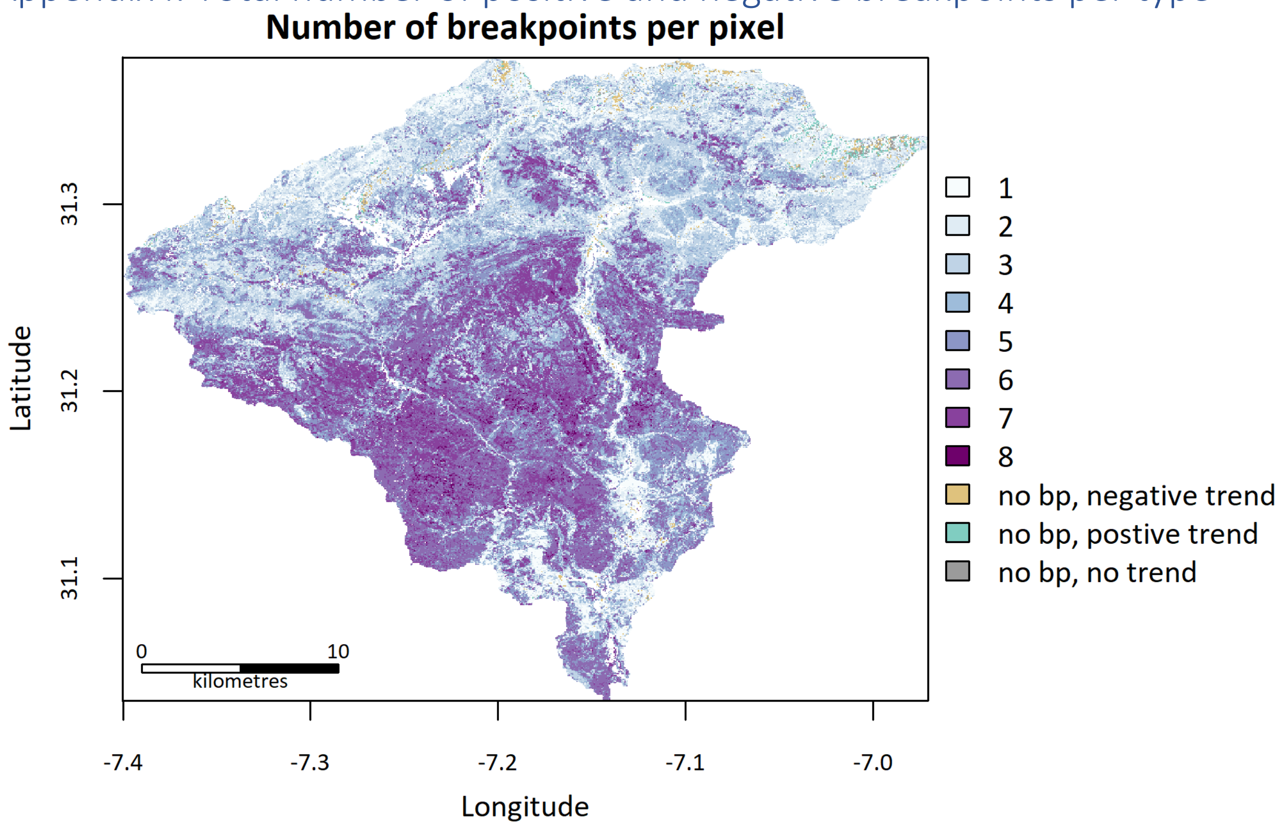

FIGURE 32 | TOTAL NUMBER OF BREAKPOINTS DETECTED PER PIXEL BETWEEN 1984 AND 2019 IN THE OUNILA WATERSHED. SPATIAL RESOLUTION IS 30 BY 30 M.

Appendix J: Mean NDVI 3 years before climatic disturbance

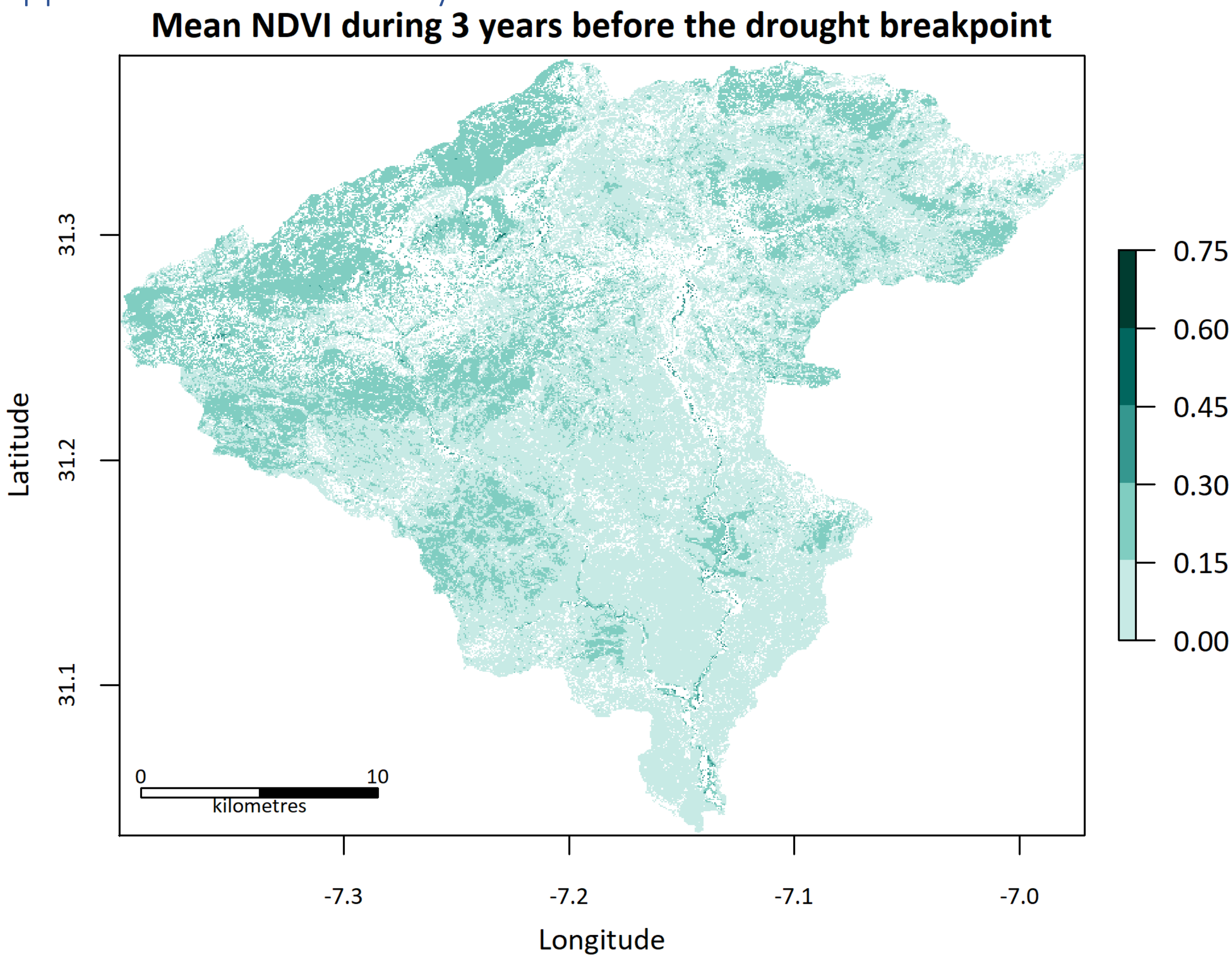

FIGURE 33 | MEAN NDVI DURING THREE YEARS BEFORE THE DROUGHT BREAKPOINT. ONLY PIXELS THAT EXPERIENCED A DROUGHT BREAKPOINT HAVE A VALUE, CROPLAND IS MASKED OUT. SPATIAL RESOLUTION IS 30 BY 30 M.

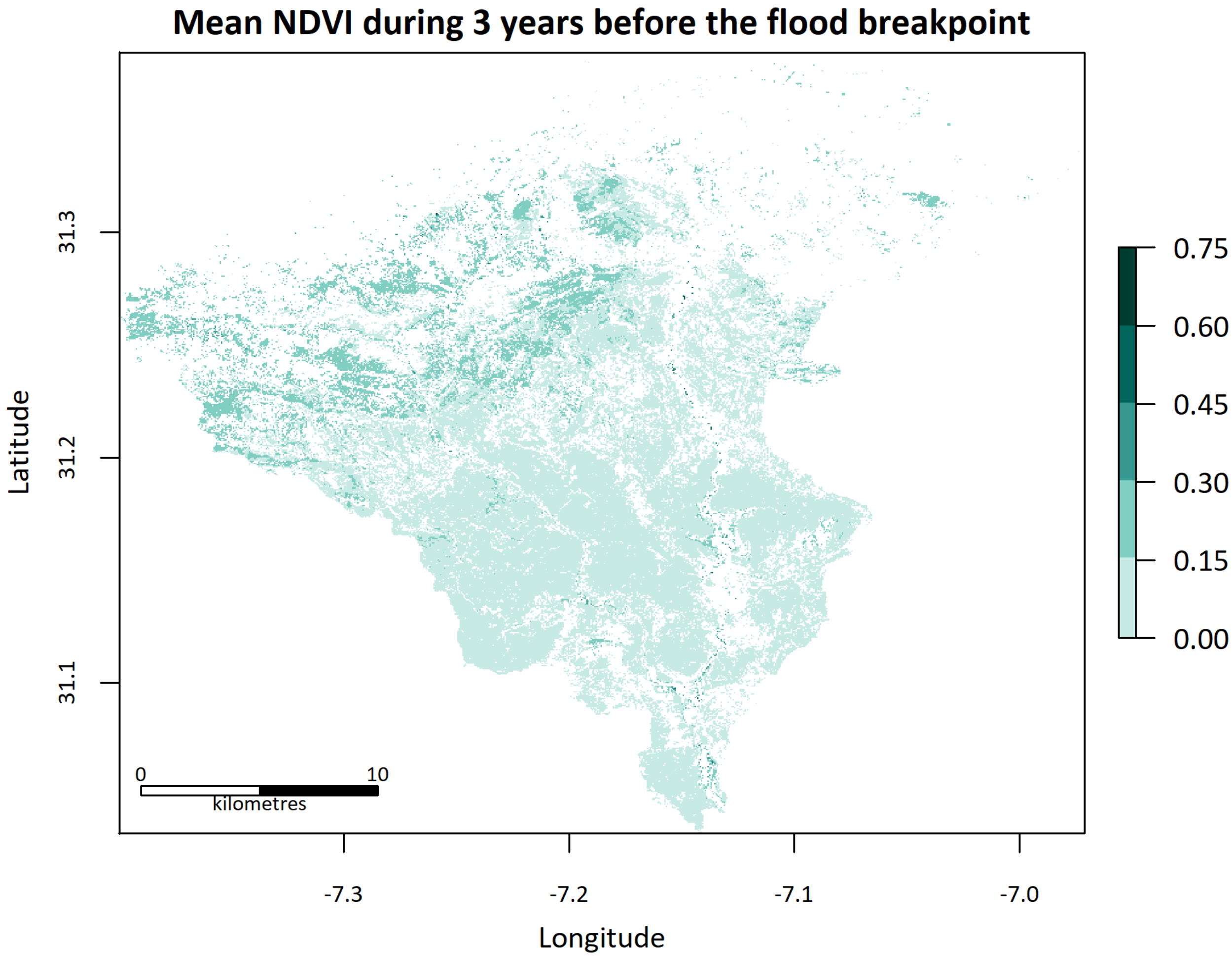

FIGURE 34 | MEAN NDVI DURING THREE YEARS BEFORE THE FLOOD BREAKPOINT. ONLY PIXELS THAT EXPERIENCED A FLOOD BREAKPOINT HAVE A VALUE, CROPLAND IS MASKED OUT. SPATIAL RESOLUTION IS 30 BY 30 M.

Appendix K: Typology of flood breakpoints and NDVI before flood

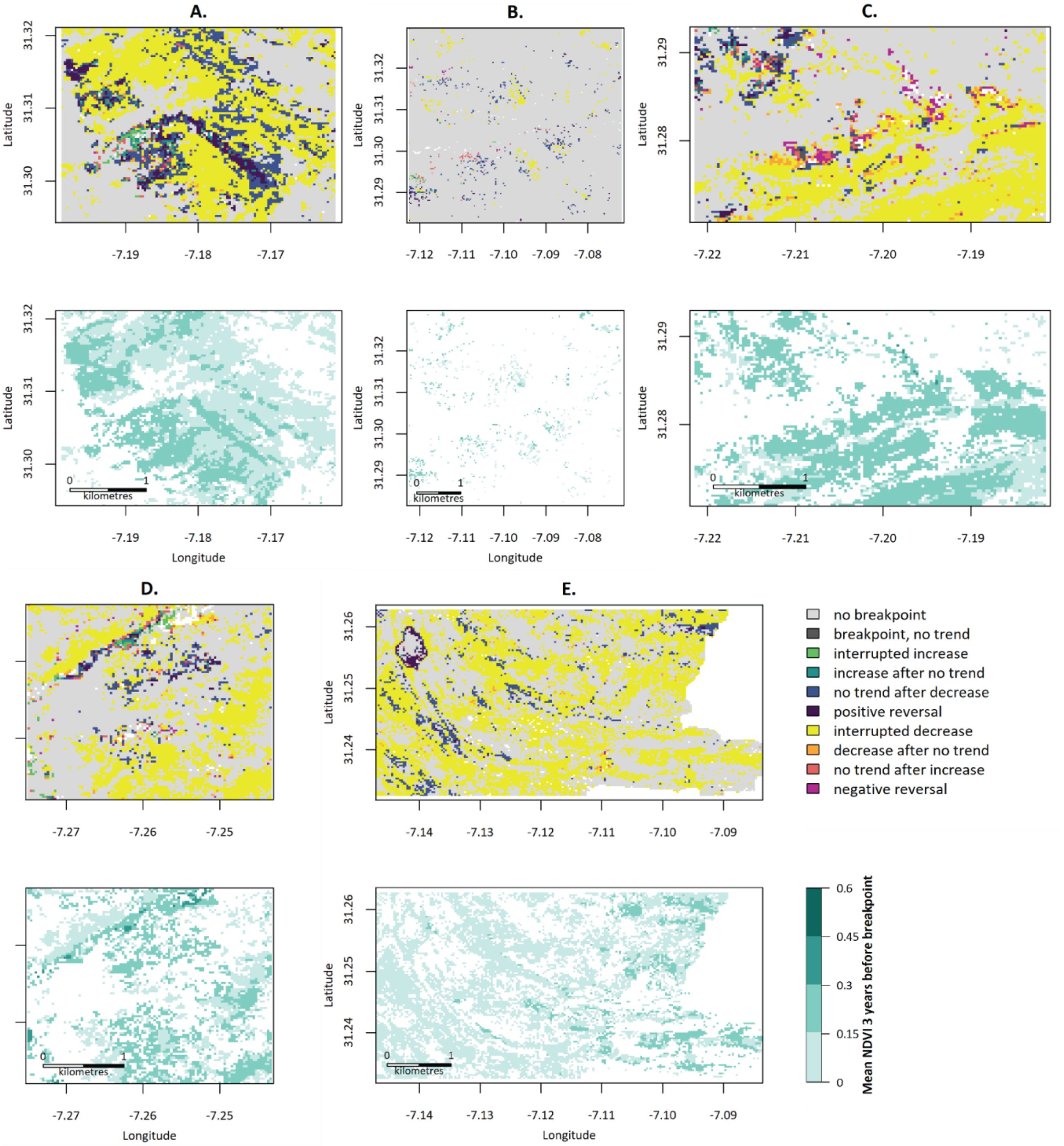

FIGURE 35 | ZOOMED IN PLOTS OF THE TYPOLOGY OF BREAKPOINTS DURING THE FLOOD AND THE MEAN NDVI DURING THREE YEARS BEFORE FLOOD BREAKPOINT FOR THE AREAS OF INTEREST: A-E. SPATIAL RESOLUTION OF IS 30 BY 30 M.